AN ABSTRACT OF THE THESIS OF

H. Dale Collins (Name) for the Ph. D. (Degree) in Electrical Engineering (Major)

Date thesis presented April 24, 1970

Title ERROR ANALYSIS IN SCANNED HOLOGRAPHY

Abstract approved by Signature redacted for privacy.
Professor R. R. Michael

Acoustic scanned holography is a method of lensless photography which uses sound waves to construct the hologram and light waves to reconstruct the image. The receiving transducer scans a plane area containing the sound field generated or scattered from the objects. In simultaneous source receiver scanning, both the source and receiver are scanned together. A cathode ray tube is used to construct the hologram and the receiver's position and velocity components are simulated electronically to control the beam position. The simulated position and velocity signals contain errors that adversely affect the quality of the images. This thesis presents an analysis of scanning errors in holography when both the receiver and source are scanned. These errors affect the hologram resolution, magnification and image position. The analysis assumes the simulated velocity and position errors are random and normally distributed. The hologram resolution, magnification and image position are derived and the functions linearized to obtain the approximate variances and expected values. The law of propagation of errors is assumed valid in the analysis. Its proof is based on the

assumption that the errors are small with respect to the measured values of the variables. The maximum deviation from the expected value is assumed never to exceed 10%.

The approximate variance, standard deviation and expected value are derived for the hologram resolution using both stationary and moving source illumination. The most exciting results were obtained by simultaneously scanning the source and receiver. The expected value of the hologram resolution is increased by a factor of two compared with the stationary source value. The variance is decreased by a factor of four with respect to the variance of the stationary source resolution. Thus, in addition to the increase in resolution there is a decrease in the standard deviation in the hologram resolution as a result of simultaneously scanning the source and receiver.

The expected value of the simultaneous source receiver scanned radial magnification was decreased by a factor of two compared with the stationary source value and the expected value of the lateral magnification remained the same. These results were unique in that scanning both the source and receiver together makes the object appear closer to the hologram plane. In other words, using the identical stationary source reconstruction geometry the image appears magnified in the lateral direction.

The expected value of the image position in the reconstruction for simultaneous source receiver scanning is equal to approximately one-half the stationary source value. If a plane wave reconstruction

source is used, the expected value of the simultaneous source receiver scanned image position is exactly half the stationary source value. The variance of the image position is less in the simultaneous source receiver scanned hologram than in the stationary source case.

A number of experiments were successfully performed to verify the theory. The experimental results of the expected values of hologram resolution, magnification and image position agreed with our predictions.

Error Analysis in Scanned Holography

by

H. D. Collins

A THESIS

submitted to

Oregon State University

in partial fulfillment of
the requirements for the
degree of

Doctor of Philosophy

June 1970

APPROVED:

Signature redacted for privacy.

Professor of Electrical Engineering

In Charge of Major

Signature redacted for privacy.

Head of Department of Electrical and Electronics Engineering

Signature redacted for privacy.

Dean of Graduate School

Date thesis is presented April 24, 1970

Typed by Linda Tipton and Judy Gelhaus

ACKNOWLEDGMENTS

The author wishes to take this opportunity to express his sincere appreciation to Professor R. R. Michael, Dr. B. P. Hildebrand, Dr. P. Magnusson, Dr. S. Nèshbya and Dr. R. D. Stalley, who served on his doctoral committee, for their suggestions and guidance. He is also indebted to R. B. Smith for his many valuable suggestions on scanned holography techniques. He also wishes to thank R. P. Gribble for his many suggestions on the experimental work.

The author is grateful to Linda Tipton for typing and Jan Sletager for editing the final copy.

The author would like to acknowledge the extreme patience and understanding by his wife Kathy Collins through the entire work.

TABLE OF CONTENTS

TABLE OF CONTENTS (Continued)

ERROR ANALYSIS IN SCANNED HOLOGRAPHY

I. INTRODUCTION

In 1948 Dennis Gabor[1,2,3,] in England proposed a method of lensless photography. He showed that by recording the intensity of the interference pattern produced by the interaction of light from the illuminated object with that of a coherent source, that the object could be reproduced in three dimensions when the pattern was illuminated with the same reference source. Gabor coined the word "hologram" to designate the film recording of the interference pattern that contained the phase and amplitude information defining the object.

In those days there were no highly coherent light sources and holography remained dormant until the laser was developed. Leith and Upatnicks[4,5,6] in 1962 modified Gabor's method of constructing holograms, so that holography with complete image separation (real and virtual) was feasible.

During the last few years holography has been applied very successfully to the field of acoustics.[7,8,9] Acoustic holography can be loosely defined as any technique that converts an acoustic field (phase and amplitude) into an optical field. The reconstruction of the acoustic hologram optically forms a visible image of the recorded object. Acoustic holography can be divided into two distinct types: scanned and liquid surface. In this thesis only scanned holography will be discussed.

In this thesis we explore the effects of position and velocity errors on the important holographic parameters. Statistical methods are used to derive approximate variances and expected or average values of the image position, radial, lateral magnifications and resolution. The analysis includes the effects of simultaneous scanning of the acoustic receiver and source.

Before proceeding with the analysis, a simple discussion of acoustic holography is necessary to provide the background for the analysis. In the next section a generalized analysis of scanned holography employing a stationary source is developed to provide the basis for the error analysis. The following sections are the derivations of the variances and expected values of the hologram parameters for stationary and moving source illumination. Finally, a description of the experiments that were performed is included to offer experimental evidence that some of the statistical parameters derived in the analysis are sound.

II. SIMPLIFIED ANALYSIS OF ACOUSTIC HOLOGRAPHY

Acoustic holography can be described as any technique for recording both the phase and amplitude of the sound reflected or scattered from an object on a medium insensitive to phase. The recorded information is then reconstructed optically to form the image of the object. The following is a brief discussion of scanned acoustic holography and the reconstruction of the true and conjugate images.

Consider the simplified acoustic hologram construction geometry as shown in Fig. 1. The object is insonafied by a point source or plane wave acoustic transmitter operating at one frequency. The scanning receiver intercepts a portion of the reflected acoustic energy from the object. The receiving transducer responds to variations in the acoustic pressure and these are generally small and superimposed on the much larger static pressure. Let the acoustic pressure in the hologram plane (due to the object) be designated as the object signal

$$S_o(x,y,t) = P_o(x,y) \cos \left[\omega t + \phi_o(x,y)\right] \tag{1}$$

where $P_o(x,y)$ is the amplitude variation,

$\phi_o(x,y)$ is the phase variation,

ω is the radian frequency of the acoustic wave, and

(x,y) defines the hologram plane.

The acoustic reference signal is simulated electronically and can be expressed as

$$S_R(t) = P_R \cos \left[\omega t + \phi_{RS}\right] \tag{2}$$

where P_R and ϕ_{RS} are arbitrary constants.

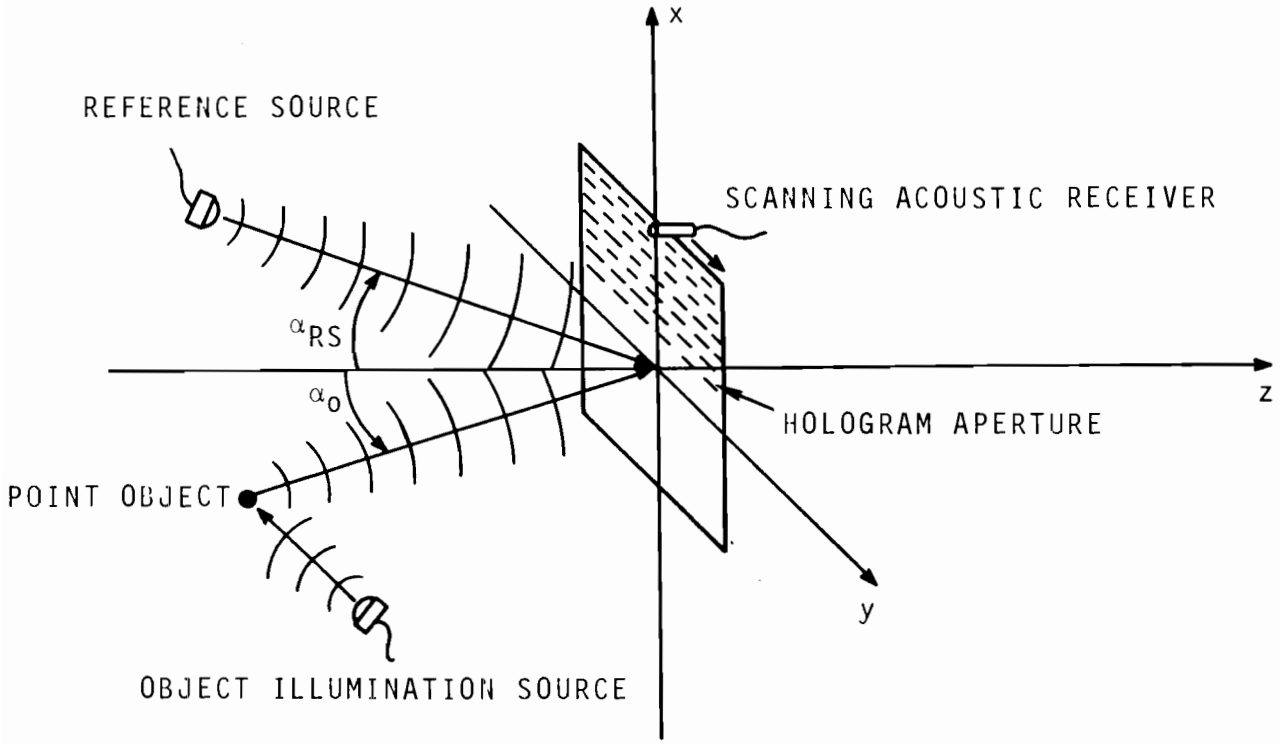

Figure 1. General acoustic hologram construction geometry.

The receiving transducer detects the resultant pressure existing at the point (x,y). The output signal of the receiver is then combined with the reference signal in a signal processor. The processor output signal is

$$S(x,y) = \frac{1}{T}\int_0^T P_o(x,y)\cos\left[\omega t + \phi_o(x,y)\right] P_R \cos\left[\omega t + \phi_{RS}\right]dt \qquad (3)$$

where

$$S(x,y) = \frac{1}{T}\int_0^T 1/2\ P_o(x,y)\ P_R \cos\left\{\left[2\omega t + \phi_o(x,y) + \phi_{RS}\right]\right.$$

$$\left. + \cos\left[\phi_o(x,y) - \phi_{RS}\right]\right\} dt \qquad (4)$$

The first term of Eq. (4) reduces to zero and the final expression is

$$S(x,y) = 1/2\ P_o(x,y)\ P_R \cos\left[\phi_o(x,y) - \phi_{RS}\right] \quad . \qquad (5)$$

In acoustical scanned holography the resultant signal, Eq. (5), is used to intensity modulate a scanning light or the CRT beam. The hologram is then constructed on the face of the oscilloscope in the latter case and directly on transparency film in the former case. The end result in either process requires the hologram to be recorded on film. The film recording of the intensity (I) is a function of its amplitude transmission characteristics. The film emulsion records some power of the intensity I(x,y), the amplitude transmittance. It is possible to obtain square-law action over a limited dynamic range with transparency film of any gamma,[10] gamma being the slope of the Hurter-Driffield curve which is a plot of the intensity transmittance versus log of the exposure. If we abandon this traditional curve and

use a direct plot of the amplitude transmittance versus exposure and bias the film at the operating point, which lies within the region of maximum linearity of the t-E curve, then over a certain dynamic range the film will provide square-law mapping of incremental changes in amplitude. Figure 2 is a typical amplitude transmittance-exposure curve for a negative transparency.

We can represent the t-E curve within this region of linearity by

$$\sqrt{\tau(x,y)} = mE + b = mI_r T + b = K|A|^2 + b \qquad (6)$$

where m is the slope of the curve at the bias point, A represents the incremental amplitude changes, and K is the product of the slope (m) and the exposure time (T). I_r is the intensity information recorded

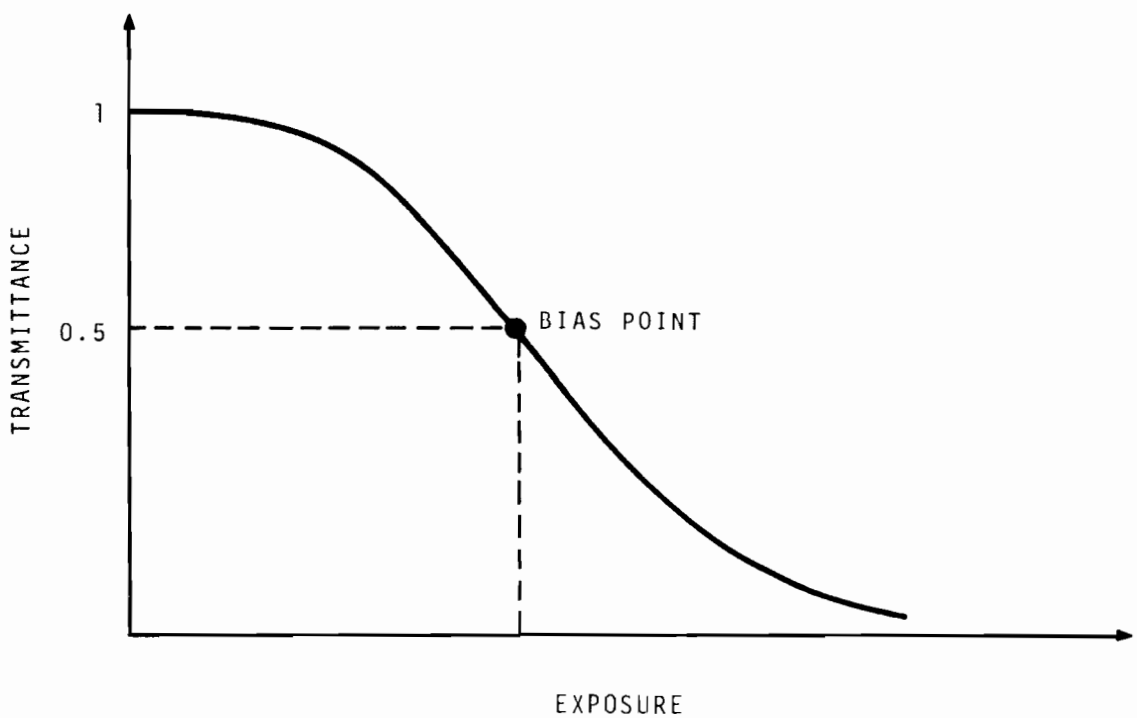

Figure 2. Typical transmittance-exposure curve for a negative transparency.

on the film in constructing the hologram. The intensity I_r is proportional to the incremental amplitude changes (i.e., $I_r = |A|^2$).

The intensity transmittance $\tau(x,y)$ of the developed transparency is defined as the ratio of the local average of the transmitted intensity at (x,y) to the incident intensity at (x,y). Using this definition the light emerging from the illuminated hologram during the reconstruction process is given by the following equation:

$$A_t(x,y) = A_i(x,y)\left\{K\, I_r(x,y) + b\right\} \tag{7}$$

where $A_t(x,y)$, $A_i(x,y)$ are the amplitudes of the transmitted and incident light.

In acoustical holography the intensity of the CRT beam or scanning light fixed to the receiver is proportional to $S(x,y) + K_1$ where K_1 is a constant proportional to the average intensity.

$$I_r(x,y) = 1/2\; P_o(x,y)\; P_R \cos\left[\phi_{RS}(x,y) - \phi_o(x,y)\right] + K_1 \quad . \tag{8}$$

The amplitude transmittance function of the film is given by the following expression

$$A_t(x,y) = A_i(x,y)\left\{1/2\; KP_o(x,y)\; P_R \cos\left[\phi_{RS}(x,y) - \phi_o(x,y)\right] + KK_1 + b\right\} \tag{9}$$

and the film described by Eq. (9) is called a hologram after Gabor.[1]

Once the amplitude and phase information about the object has been recorded, there remains to reconstruct the image of the object. If we

illuminate the developed transparency (i.e., the hologram) with a point source of monochromatic light derived from a laser, then

$$A_i(x,y) = A_1 \cos\left[\omega_L t + \phi_{RL}(x,y)\right] \tag{10}$$

where the light emerging from the hologram is given by Eq. (7).

$$A_t(x,y) = A_1 \cos\left(\omega_L t + \phi_{RL}\right)\left\{1/2\ KP_o(x,y)\ P_R \cos\left[\phi_{RS}(x,y) - \phi_o(x,y)\right] + KK_1 + b\right\} \quad . \tag{11}$$

Using a trigonometric identity, Eq. (11) can be expressed as

$$A_t(x,y) = 1/4\ KA_1\ P_o(x,y)\ P_R \cos\left[\omega_L t + \phi_o(x,y) + \phi_{RL}(x,y) - \phi_{RS}(x,y)\right] + 1/4\ KA_1\ P_o(x,y)\ P_R \cos\left[\omega_L t + \phi_{RL}(x,y) + \phi_{RS}(x,y) - \phi_o(x,y)\right] A_1(KK_1 + b) \cos\left[\omega_L t + \phi_{RL}(x,y)\right] \quad . \tag{12}$$

The first term of Eq. (12) indicates that it is of the same form as the original object signal, Eq. (1), except for the amplitude weighting $1/2\ KA_1\ P_R$ and the phase terms ϕ_{RL} and ϕ_{RS}. This implies that the sound which was reflected or scattered by the object would be reproduced exactly if the phase terms $\phi_{RS}(x,y)$ and $\phi_{RL}(x,y)$ were equal. To analyze this imposed requirement, we can express the phase terms of Eq. (12) by the following expressions

$$\phi_o(x,y) = \phi_o'(x,y) + \frac{2\pi}{\lambda_s} x \sin \bar{\alpha}_o \quad , \tag{13}$$

$$\phi_{RL}(x,y) = \phi_{RL}'(x,y) + \frac{2\pi}{\lambda_L} x \sin \bar{\alpha}_{RL} \quad , \tag{14}$$

$$\phi_{RS}(x,y) = \phi_{RS}'(x,y) + \frac{2\pi}{\lambda_S} x \sin \bar{\alpha}_{RS} \quad , \tag{15}$$

if the reference, object and reconstruction signals are assumed to be plane waves. The above terms take into account the phase variations about the average angular deviations $\bar{\alpha}_o$, $\bar{\alpha}_{RS}$, $\bar{\alpha}_{RL}$ and the phase variations $\phi_o(x,y)$, $\phi_{RL}(x,y)$, $\phi_{RS}(x,y)$, at the hologram plane. The analysis assumes that the object and reference positional variations occur in the x-z plane only (see Figs. 1, 3 and 4).

If the phase terms $\phi_{RS}(x,y)$ and $\phi_{RL}(x,y)$ are to be equal, then the following conditions must be satisfied:

$$\sin \bar{\alpha}_{RL} = \frac{\lambda_L}{\lambda_S} \sin \bar{\alpha}_{RS} \quad , \tag{16}$$

$$\phi'_{RL}(x,y) = \phi'_{RS}(x,y) \quad . \tag{17}$$

The ratio of the light to acoustic wavelengths $^{\lambda}L/^{\lambda}S$ is usually very small in most applications. For example, suppose we employ a helium-neon laser for the source in reconstructing the acoustic hologram that was constructed using 1 MHz sound. The ratio $^{\lambda}L/^{\lambda}S$ is approximately 4×10^{-4}. This means the acoustic reference signal can be simulated almost without regard to the direction angle $\bar{\alpha}_{RS}$ requirement because the reconstruction source angle $\bar{\alpha}_{RL}$ is essentially zero for all values of $\bar{\alpha}_{RS}$. This condition restricts the direction of the reconstruction beam to be essentially perpendicular to the hologram plane as shown in Figs. 3 and 4.

If we now substitute Eqs. (13), (14), and (15) into Eq. (12) and assume the phase terms $\phi_{RS}(x,y)$, $\phi_{RL}(x,y)$ are equal, then the final expression for the light emerging from the hologram in the reconstruction process is

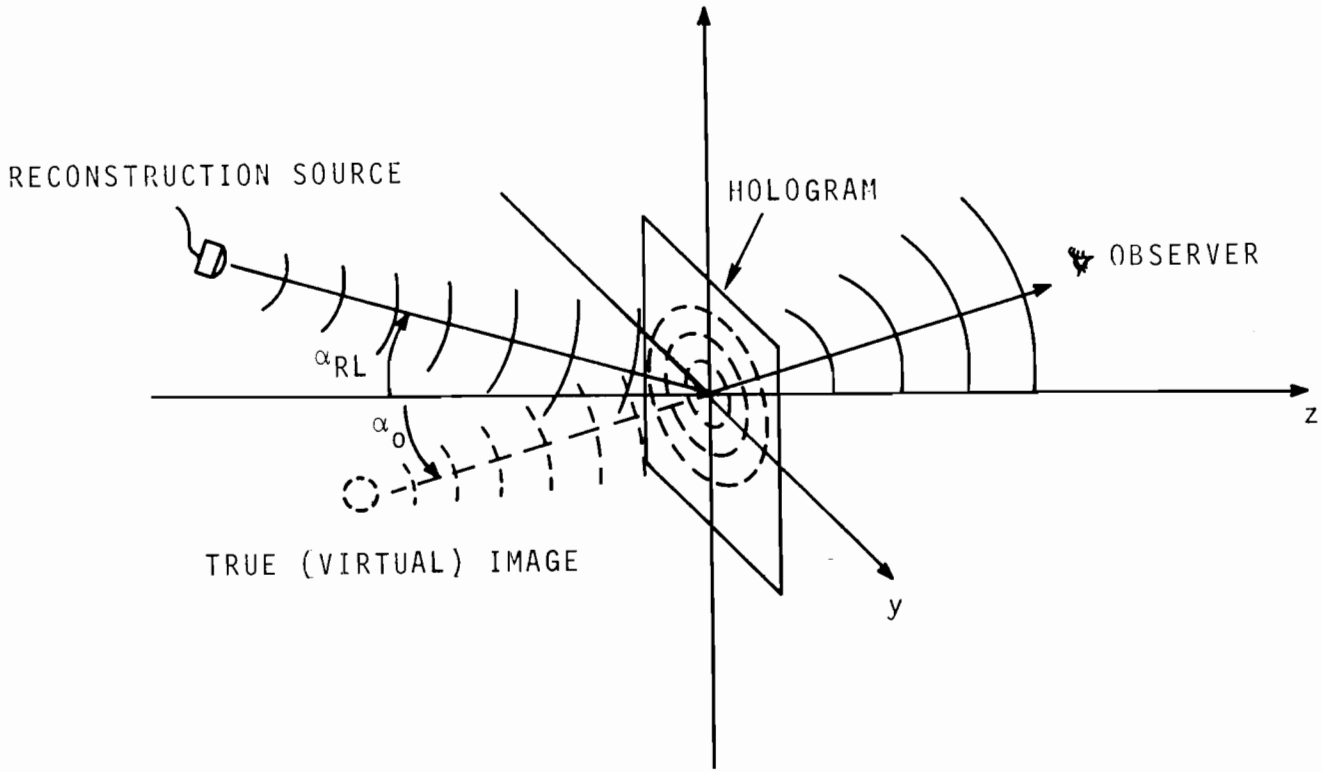

Figure 3. General reconstruction geometry for the true image.

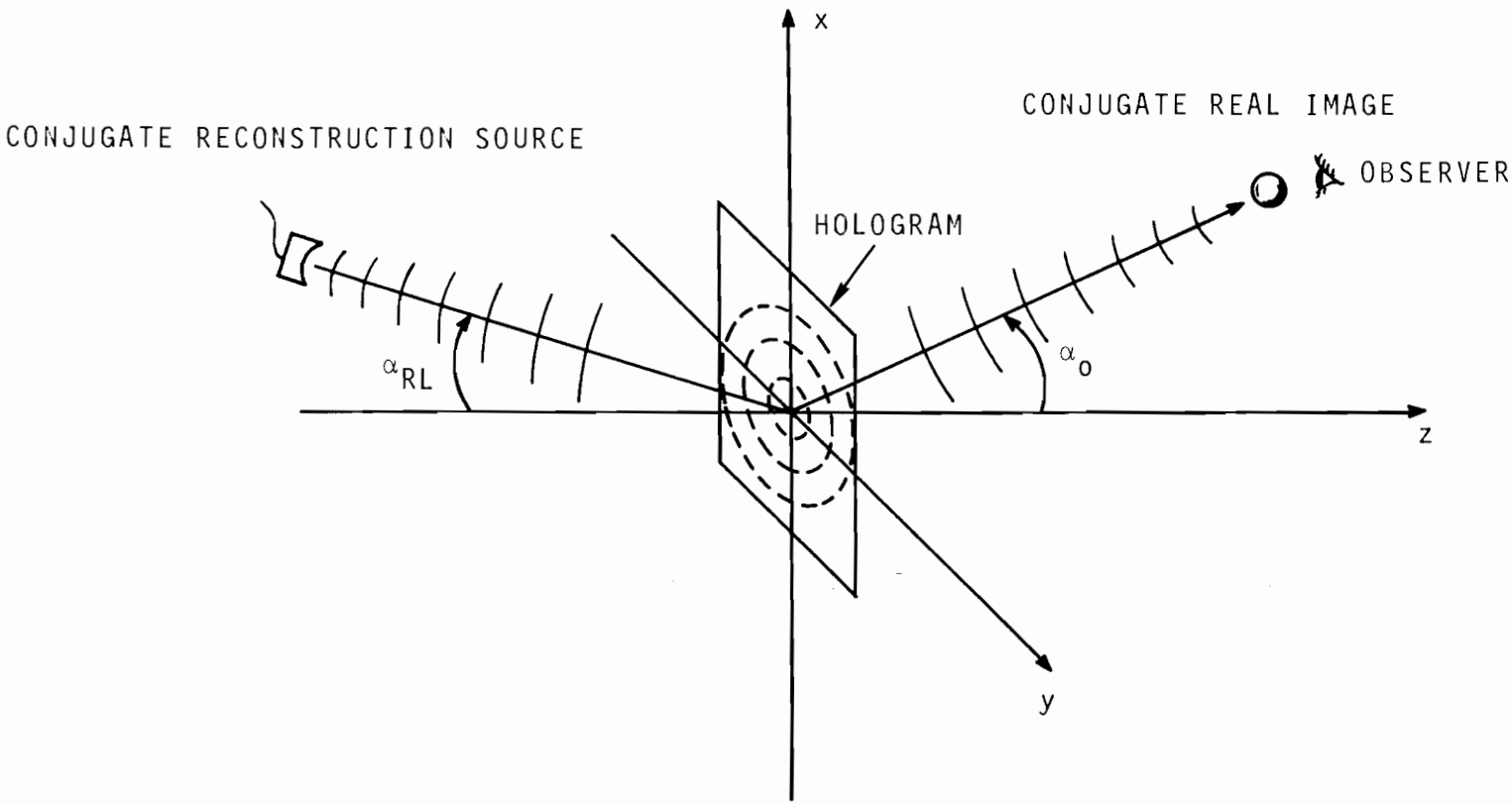

Figure 4. General reconstruction geometry for the conjugate image.

$$A_t(x,y) = 1/4\ KA_1\ P_o(x,y)\ P_R \cos\left[\omega_L t + \phi_o(x,y)\right]$$

$$+ 1/4\ KA_1\ P_o(x,y)\ P_R \cos\left[\omega_L t + \phi_{RL}(x,y) + \phi_{RS}(x,y) - \phi_o(x,y)\right]$$

$$+ (KK_1 + b)\ A_1 \cos\left[\omega_L t + \phi_{RL}\right] \quad . \tag{18}$$

Notice, that the first term in Eq. (18) is simply an exact duplication of the original object signal Eq. (1) except for amplitude weighting. In the reconstruction the diffracted light due to the first term appears to the observer as the true virtual image of the object as shown in Fig. 3. The direction of propagation of the image is about the average angle $\bar{\alpha}_o$. The second term is referred to as the conjugate image. The conjugate image is propagated at a different angle than the true image and therefore, does not interfere with it in the reconstruction. The third term is simply the reconstruction beam with amplitude weighting. It is commonly referred to as the dc term.

If we wish to observe the conjugate image, we illuminate the hologram with a reconstruction source which can be expressed as

$$A_i(x,y) = A_1 \cos\left[\omega_L t - \phi_{RL}(x,y)\right] \tag{19}$$

where $\phi_{RL}(x,y)$ is equal to $\phi_{RS}(x,y)$. The light emerging from the hologram can be expressed as

$$A_t(x,y) = 1/4\ KA_1\ P_o(x,y)\ P_R \cos\left[\omega_L t - \phi_o(x,y)\right]$$

$$+ 1/4\ KA_1\ P_o(x,y)\ P_R \cos\left[\omega_L t + \phi_{RL}(x,y) + \phi_{RS}(x,y) - \phi_o(x,y)\right]$$

$$+ (KK_1 + b)\ A_1 \cos\left[\omega_L t - \phi_{RL}(x,y)\right] \tag{20}$$

where the first term represents the conjugate image of the object. This is a pseudo-image because the phase information is reversed (i.e., the object appears inside out). The conjugate image appears at a mean angle $-\bar{\alpha}_0$ and this places it on the side of the hologram opposite to the reconstruction source. Thus, it is a real conjugate image of the object as shown in Fig. 4.

III. GENERALIZED ANALYSIS OF SCANNED ACOUSTIC HOLOGRAPHY

The analysis in the preceeding section was intended to present a simplified analysis of the basic construction and reconstruction process in acoustical scanned holography. To determine the effects of random position and velocity errors introduced by the scanning receiver (either mechanical and electrical) in acoustical holography on the important holographic parameters such as image location, resolution, radial and lateral magnification, a detailed analysis will be carried out. This analysis of holography uses an analytic technique similar to that used by K. Haines and Kogo Kamiya.[11]

The hologram construction and reconstruction geometry used in this analysis is illustrated in Fig. 5. The position of the fringes on the hologram plane that are constructed by interference of the reference electronic signal (i.e., simulated plane wave source) and the reflected signal from the object can be expressed as

$$\beta_S \left[r_0 + r_1 - r_2 \right] = 2n\pi$$

and

$$\beta_S = \frac{2\pi}{\lambda_S} \tag{21}$$

where λ_S is the wavelength used for the construction of the hologram and n is an integer. We will assume the hologram to be recorded on film which consists of opaque or transparent sections whenever Eq. (21) is satisfied. The effect of replacing the actual hologram film with this approximate one would be a construction of images of all orders. We will consider only the first order diffracted image, since in

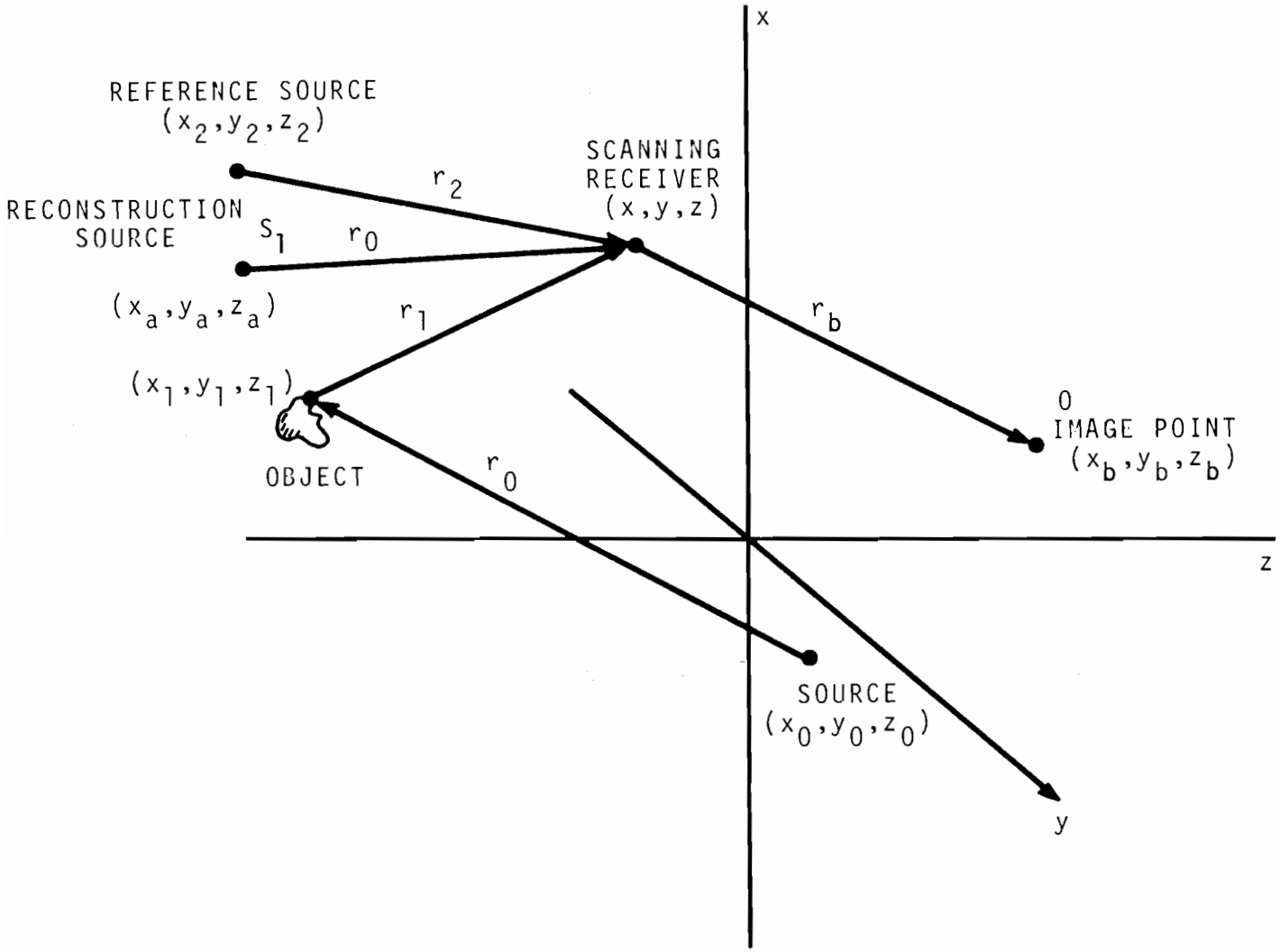

Figure 5. Acoustic hologram geometry.

reality the actual hologram will allow no other recognizable images. If an image is to be formed at O, then the light from S_1 passing through the hologram film and arriving at the image point O must be in phase. This can be expressed as

$$\beta_L \left[r_a + r_b \right] = \pm 2\pi n + \beta_L C \tag{22}$$

and

$$\beta_L = 2\pi/\lambda_L$$

where C is a constant defined as the optical path function, and λ_L is the wavelength of the reconstruction source. We may substitute for n from Eq. (21) into Eq. (22) and obtain the following expression:

$$\beta_L \left[r_a + r_b \right] = \pm \beta_S \left[r_0 + r_1 - r_2 \right] + \beta_L C \tag{23}$$

Since C is a constant, the differential of C with respect to x or y should be zero. If $\frac{\partial C}{\partial x}$ and $\frac{\partial C}{\partial y}$ are zero without any restrictions, then a perfect image will be formed at O. This is essentially Fermat's principle, which states the position of image point O for the ray from S_1 should be where the variation of the optical path function C becomes zero. This implies that the position of the image at O for a ray from S is where the variation of the optical path function C is zero. In reality, the differentials $\frac{\partial C}{\partial x}$, $\frac{\partial C}{\partial y}$ are not zero at the point and only become approximately zero under the following conditions. First, we express the distance terms r_a, r_b, r_0, r_1 and r_2 of Eq. (23) in rectangular coordinates:

$$\pm \beta_S \left\{ \left[(x_1 - x)^2 + (y_1 - y)^2 + z_1^2 \right]^{1/2} \right.$$

$$+ \left[(x_0 - x_1)^2 + (y_0 - y_1)^2 + z_0 - z_1)^2 \right]^{1/2}$$

$$\left. - \left[(x_2 - x)^2 + (y_2 - y)^2 + z_2^2 \right]^{1/2} \right\}$$

$$+ \beta_L C = \beta_L \left\{ \left[(x_a - x)^2 + (y_a - y)^2 + z_a^2 \right]^{1/2} \right.$$

$$\left. + \left[(x_b - x)^2 + (y_b - y)^2 + z_b^2 \right]^{1/2} \right\} \quad . \tag{24}$$

In the construction process the receiver's "x" component of velocity is denoted by v_x and the "y" component by v_y. The receiver's position at any time "t" in the construction process can be defined mathematically by the following equations:

$$x = v_x t \quad , \tag{25}$$

$$y = v_y t \quad . \tag{26}$$

The position of the CRT beam which simulates the actual receiver position can be defined in terms of its ξ and η coordinates. The ξ and η velocity components of the scanning beam are defined by the following equations:

$$\xi = v_\xi t \quad , \tag{27}$$

$$\eta = v_\eta t \quad . \tag{28}$$

Substituting Eqs. (27) and (28) into Eqs. (25) and (26), we arrive with the following expressions for x and y:

$$x = m_x \xi \quad , \tag{29}$$

$$y = m_y \eta \quad , \tag{30}$$

where

$$m_x = \frac{v_x}{v_\xi} \tag{31}$$

and

$$m_y = \frac{v_y}{v_\eta} \quad . \tag{32}$$

In reality, the differentials $\frac{\partial C}{\partial \xi}$ and $\frac{\partial C}{\partial \eta}$ become zero at a point only if a small region is considered around O. It is this small region which yields the equations relating to aberrations. If ξ and η are small, then the distance terms in Eq. (24) can be approximated. We substitute Eqs. (29) and (30) into Eq. (24) and expand the distance terms in a binominal expansion

$$\beta_L C = \beta_L \left\{ \bar{r}_a \left[1 - \frac{(\xi x_a + \eta y_a)}{\bar{r}_a^2} + \frac{\xi^2 + \eta^2}{2\bar{r}_a^2} - \frac{(\xi x_a + \eta y_a)^2}{2\bar{r}_a^4} \right.\right.$$

$$\left. - \frac{(\xi^2 + \eta^2)^2}{8\bar{r}_a^4} + \frac{(\xi^2 + \eta^2)(\xi x_a + \eta y_a)}{2\bar{r}_a^4} \right]$$

$$+ \bar{r}_b \left[1 - \frac{(\xi x_b + \eta y_b)}{2\bar{r}_b^2} + \frac{\xi^2 + \eta^2}{2\bar{r}_b^2} - \frac{(\xi x_b + \eta y_b)^2}{2\bar{r}_b^4} - \frac{(\xi^2 + \eta^2)^2}{8\bar{r}_b^4} \right.$$

$$\left. \left. + \frac{(\xi^2 + \eta^2)(\xi x_b + \eta y_b)}{2\bar{r}_b^4} \right] \right\} \mp \beta_S \left\{ \bar{r}_1 \left[1 - \frac{(m_x \xi x_1 + m_y \eta y_1)}{\bar{r}_1^2} \right.\right.$$

$$+ \frac{m_x^2 \xi^2 + m_y^2 \eta^2}{2\bar{r}_1^2} - \frac{(m_x \xi x_1 + m_y \eta y_1)^2}{2\bar{r}_1^4}$$

$$\left. - \frac{(m_x^2 \xi^2 + m_y^2 \eta^2)^2}{8\bar{r}_1^4} + \frac{(m_x^2 \xi^2 + m_y^2 \eta^2)(m_x \xi x_1 + m_y \eta y_1)}{2\bar{r}_1^4} \right]$$

$$- \bar{r}_2 \left[1 - \frac{(m_x \xi x_2 + m_y \eta y_2)}{\bar{r}_2^2} + \frac{m_x^2 \xi^2 + m_y^2 \eta^2}{2\bar{r}_2^2} - \frac{(m_x \xi x_2 + m_y \eta y_2)^2}{2\bar{r}_2^4} \right.$$

$$\left. - \frac{(m_x^2 \xi^2 + m_y^2 \eta^2)^2}{8\bar{r}_2^4} + \frac{(m_x^2 \xi^2 + m_y^2 \eta^2)(m_x \xi x_2 + m_y \eta y_2)}{2\bar{r}_2^4} \right] + r_0 \Bigg\} \tag{33}$$

where

$$\bar{r}_1^2 = x_1^2 + y_1^2 + z_1^2 \quad ,$$

$$\bar{r}_2^2 = x_2^2 + y_2^2 + z_2^2 \quad ,$$

$$\bar{r}_a^2 = x_a^2 + y_a^2 + z_a^2 \quad ,$$

$$\bar{r}_b^2 = x_b^2 + y_b^2 + z_b^2 \quad .$$

We may now combine all of these terms and express C as:

$$C = \left[\bar{r}_a + \bar{r}_b \mp \frac{\lambda_L}{\lambda_S} \bar{r}_1 \pm \frac{\lambda_L}{\lambda_S} \bar{r}_2 \pm \frac{\lambda_L}{\lambda_S} r_0 \right]$$

$$- \left[\frac{\xi x_a + \eta y_a}{\bar{r}_a} + \frac{\xi x_b + \eta y_b}{\bar{r}_b} \mp \frac{\lambda_L}{\lambda_S} \frac{(m_x \xi x_1 + m_y \eta y_1)}{\bar{r}_1} \right.$$

$$\left. \pm \frac{\lambda_L}{\lambda_S} \frac{(m_x \xi x_2 + m_y \eta y_2)}{\bar{r}_2} \right]$$

$$+ \frac{1}{2} (\xi^2 + \eta^2) \left[\frac{1}{\bar{r}_a} + \frac{1}{\bar{r}_b} \right] \mp \frac{1}{2} \frac{\lambda_L}{\lambda_S} (m_x^2 \xi^2 + m_y^2 \eta^2) \left[\frac{1}{\bar{r}_1} - \frac{1}{\bar{r}_2} \right]$$

$$- \frac{1}{2}\left[\frac{(\xi x_a + \eta y_a)^2}{\bar{r}_a^3} + \frac{(\xi x_b + \eta y_b)^2}{\bar{r}_b^3} \mp \frac{\lambda_L}{\lambda_S}\frac{(m_x\,\xi x_1 + m_y\,\eta y_1)^2}{\bar{r}_1^3} \pm \frac{\lambda_L}{\lambda_S}\frac{(m_x\,\xi x_2 + m_y\,\eta y_2)^2}{\bar{r}_2^3}\right]$$

$$+ \frac{1}{2}\,\xi(\xi^2 + \eta^2)\left[\frac{x_a}{\bar{r}_a^3} + \frac{x_b}{\bar{r}_b^3}\right] \mp \frac{\lambda_L}{\lambda_S}\frac{1}{2}\,m_x\,\xi(m_x^2\,\xi^2 + m_y^2\,\eta^2)\left[\frac{x_1}{\bar{r}_1^3} - \frac{x_2}{\bar{r}_2^3}\right]$$

$$+ \frac{1}{2}\,\eta(\xi^2 + \eta^2)\left[\frac{y_a}{\bar{r}_a^3} + \frac{y_b}{\bar{r}_b^3}\right] \mp \frac{\lambda_L}{\lambda_S}\frac{1}{2}\,m_y\,\eta(m_x^2\,\xi^2 + m_y^2\,\eta^2)\left[\frac{y_1}{\bar{r}_1^3} - \frac{y_2}{\bar{r}_2^3}\right]$$

$$- \frac{1}{8}(\xi^2 + \eta^2)^2\left[\frac{1}{\bar{r}_a^3} + \frac{1}{\bar{r}_b^3}\right] \pm \frac{1}{8}\frac{\lambda_L}{\lambda_S}(m_x^2\,\xi^2 + m_y^2\,\eta^2)^2\left[\frac{1}{\bar{r}_1^3} - \frac{1}{\bar{r}_2^3}\right] . \quad (34)$$

The differentials of C with respect to ξ and η are

$$\frac{\partial C}{\partial \xi} = -\left[\frac{x_a}{\bar{r}_a} + \frac{x_b}{\bar{r}_b} \mp \frac{\lambda_L}{\lambda_S}\frac{m_x\,x_1}{\bar{r}_1} \pm \frac{\lambda_L}{\lambda_S}\frac{m_x\,x_2}{\bar{r}_2}\right] + \xi\left[\frac{1}{\bar{r}_a} + \frac{1}{\bar{r}_b}\right]$$

$$\mp \frac{\lambda_L}{\lambda_S}\,m_x^2\,\xi\left[\frac{1}{\bar{r}_1} - \frac{1}{\bar{r}_2}\right] + \frac{\partial}{\partial \xi}\ (\text{higher order terms}) = 0 \quad (35)$$

and

$$\frac{\partial C}{\partial \eta} = -\left[\frac{y_a}{\bar{r}_a} + \frac{y_b}{\bar{r}_b} \mp \frac{\lambda_L}{\lambda_S}\frac{m_y\,y_1}{\bar{r}_1} \pm \frac{\lambda_L}{\lambda_S}\frac{m_y\,y_2}{\bar{r}_2}\right] + \eta\left[\frac{1}{\bar{r}_a} + \frac{1}{\bar{r}_b}\right]$$

$$\mp \frac{\lambda_L}{\lambda_S}\,m_y^2\,\eta\left[\frac{1}{\bar{r}_1} - \frac{1}{\bar{r}_2}\right] + \frac{\partial}{\partial \eta}\ (\text{higher order terms}) = 0 \quad . \quad (36)$$

Equations (35) and (36) do not become zero because of the higher order terms in the expansion. These terms contain the aberrations of the system. If the hologram aperture is reduced to a point, the aberrations will disappear. The above differentials will be used to derive the Gaussian image location equations.

IMAGE LOCATION EQUATIONS

To solve for the Gaussian image location equations, we assume the hologram aperture dimensions are small compared with the distances z_1, z_2, z_0 and centered around the (x,y,z) origin. In the coordinate transformation it is centered about the (ξ,η,γ) origin. The result of this condition is to restrict the scanning receiver to small excursions about the (x,y,z) origin and a degradation of the resolution. The higher order terms of Eqs. (35) and (36) can now be neglected. If C is constant, then the differentials $\frac{\partial C}{\partial \xi}$ and $\frac{\partial C}{\partial \eta}$ must be zero. Setting Eqs. (35) and (36) equal to zero and equating coefficients in ξ and η, we generate the following image location equations for the receiver scanning alone.

$$\frac{x_b}{\bar{r}_b} = \pm \frac{\lambda_L}{\lambda_S}\left(\frac{v_x}{v_\xi}\right)\left[\frac{x_1}{\bar{r}_1} - \frac{x_2}{\bar{r}_2}\right] - \frac{x_a}{\bar{r}_a} \quad , \tag{37}$$

$$\frac{y_b}{\bar{r}_b} = \pm \frac{\lambda_L}{\lambda_S}\left(\frac{v_y}{v_\eta}\right)\left[\frac{y_1}{\bar{r}_1} - \frac{y_2}{\bar{r}_2}\right] - \frac{y_a}{\bar{r}_a} \quad , \tag{38}$$

$$\frac{1}{\bar{r}_b} = \pm \frac{\lambda_L}{\lambda_S}\left(\frac{v_x}{v_\xi}\right)^2\left[\frac{1}{\bar{r}_1} - \frac{1}{\bar{r}_2}\right] - \frac{1}{\bar{r}_a} \quad , \tag{39}$$

$$\frac{1}{\bar{r}_b} = \pm \frac{\lambda_L}{\lambda_S} \left(\frac{v_y}{v_\eta}\right)^2 \left[\frac{1}{\bar{r}_1} - \frac{1}{\bar{r}_2}\right] - \frac{1}{\bar{r}_a} \quad . \tag{40}$$

The upper signs refer to the conjugate images and the lower signs refer to the true images.

MAGNIFICATIONS

The stationary source or receiver scanning alone hologram radial and lateral magnifications are given by the following expressions:

Radial $$M_R = \pm \frac{\partial \bar{r}_b}{\partial r_1} = \pm \frac{\lambda_L}{\lambda_S} \left(\frac{\bar{r}_b}{r_1}\right)^2 \left(\frac{V_x}{V_\xi}\right)^2 \quad , \tag{41}$$

Lateral $$M_{L_{(x)}} = \pm \frac{\partial x_b}{\partial x_1} = \pm \frac{\lambda_L}{\lambda_S} \left(\frac{\bar{r}_b}{r_1}\right)\left(\frac{V_x}{V_\xi}\right) \quad , \tag{42}$$

$$M_{L_{(y)}} = \pm \frac{\partial y_b}{\partial y_1} = \pm \frac{\lambda_L}{\lambda_S} \left(\frac{\bar{r}_b}{r_1}\right)\left(\frac{V_y}{V_\eta}\right) \quad . \tag{43}$$

If the details of source receiver scanning for the more general cases of acoustic holography are to be understood, then a more complete analysis is in order. Such an analysis is carried out in Appendix B.

IV. RESOLUTION ERRORS IN ACOUSTIC HOLOGRAPHY

The resolution in the object space is defined as the incremental distance Δx_1 through which the object point can be displaced before the phase of the finest fringe arising at the hologram plane is deviated π radians during the recording process.[12]

The phase at the receiving transducer in the hologram plane during the recording process is

$$\phi_1(x,y,z) = \frac{2\pi}{\lambda_S}\left[r_0 + r_1 - r_2\right] \quad . \tag{44}$$

If the phase $\phi_1(x,y,z)$ varies at a rate $\frac{\partial \phi_1}{\partial x_1}(x,y,z)$, then the incremental phase change when the object point moves an incremental distance Δx_1 is

$$\Delta\phi_1(x,y,z) = \frac{\partial \phi_1}{\partial x_1}(x,y,z)\ \Delta x_1 \tag{45}$$

where

$$\Delta\phi_1(x,y,z) = \frac{2\pi}{\lambda_S}\left\{\frac{(x_1 - x)}{\left[(x_1 - x)^2 + (y_1 - y)^2 + (z_1 - z)^2\right]^{1/2}} + \frac{(x_1 - x_0)}{\left[(x_1 - x_0)^2 + (y_1 - y_0)^2 + (z_1 - z_0)^2\right]^{1/2}}\right\}\Delta x_1 \quad . \tag{46}$$

Setting Eq. (46) equal to π and solving for the resolution Δx_1, we obtain the following expression:

$$\Delta x_1 = \frac{\lambda_S}{2\left[\frac{(x_1 - x)}{r_1} + \frac{(x_1 - x_0)}{r_0}\right]} \quad . \tag{47}$$

Let v_x and v_y be the actual acoustic receiver velocity components in the recording aperture (i.e., (x,y) plane) and v_ξ, v_η the simulated velocity components. The ξ, η coordinates are related to the x,y coordinates by the following equations:

$$x = m_x \xi \tag{48}$$

$$y = m_y \eta \tag{49}$$

We now substitute Eqs. (48) and (49) into Eq. (47) and assume that random errors exist in the simulated position of the acoustic receiver during the hologram construction. The following linear statistical models are used

$$\xi = \bar{\xi} + e_\xi \tag{50}$$

$$\eta = \bar{\eta} + e_\eta \tag{51}$$

where $\bar{\xi}$ and $\bar{\eta}$ are the mean values and e_ξ and e_η are statistically independent random errors. It is assumed that the errors are normally distributed with zero means and their respective variances (σ_ξ^2, σ_η^2). In order to derive the variance and expected value of the stationary source hologram resolution, we expand the function (Δx_1) in a Taylor's series. If the errors e_ξ and e_η are small with respect to the measured values of the independent variables ξ and η (i.e., σ_ξ and σ_η < 0.1 of ξ and η, respectively), then only the linear terms of the expansion are retained (see Appendices A and B). This approximation is usually quite adequate for obtaining the approximate variance and expected value of an arbitrary function. The final expression for the linear terms is given by the following equation:

$$\Delta x_1 \cong \frac{\lambda_s}{\frac{2(x_1-m_x\,\bar{\xi})}{r_1}+\frac{2(x_1-x_0)}{r_0}} + m_x\,\frac{\lambda_s}{2}\,\frac{r_0}{r_1}\left\{\frac{r_1^{\,2}\,r_0-(x_1-m_x\,\bar{\xi})^2}{\left[r_0(x_1-m_x\bar{\xi})+r_1(x_1-x_0)\right]^2}\right\}(\xi-\bar{\xi})$$

$$+\,m_y\,\frac{\lambda_s}{2}\,\frac{r_0}{r_1}\left\{\frac{r_0(m_y\bar{\eta}-y_1)\,(x_1-m_x\bar{\xi})}{\left[r_0\,(x_1-m_x\bar{\eta})+r_1(x_1-x_0)\right]^2}\right\}(\eta-\bar{\eta}) \qquad (52)$$

where

$$r_1=\sqrt{(x_1-m_x\,\bar{\xi})^2+(y_1-m_y\,\bar{\eta})^2+z_1^{\,2}}\quad . \qquad (53)$$

VARIANCE OF THE STATIONARY SOURCE HOLOGRAM RESOLUTION

The variance of the stationary source hologram resolution Δx_1 when statistically independent random errors are introduced is

$$V\left[\Delta x_1\right]_{ss}=\left(\frac{\lambda_s}{2}\,\frac{r_0}{r_1}\,m_x\right)^2\left\{\frac{r_1^{\,2}\,r_0-r_0(x_1-m_x\,\bar{\xi})^2}{\left[r_0(x_1-m_x\,\bar{\xi})+r_1(x_1-x_0)\right]^2}\right\}^2\sigma_\xi^{\,2}$$

$$+\left(\frac{\lambda_s}{2}\,\frac{r_0}{r_1}\,m_x\right)^2\left\{\frac{r_0(m_y\,\bar{\eta}-y_1)\,(x_1-m_x\,\bar{\xi})}{\left[r_0(x_1-m_x\,\bar{\xi})+r_1(x_1-x_0)\right]^2}\right\}^2\sigma_\eta^{\,2} \qquad (54)$$

If the deviations in the simulated receiver positions are assumed never to exceed three standard deviations, then estimators of the variances can be defined as

$$\hat{\sigma}_\xi^{\,2}=\frac{\Delta\xi^2}{9} \qquad (55)$$

$$\hat{\sigma}_\eta^{\,2}=\frac{\Delta\eta^2}{9} \qquad (56)$$

This assumes the maximum deviation of errors in the ξ and η scanning receiver positions will essentially never exceed these values. The

probability of errors greater than $\Delta\xi$ or $\Delta\eta$ is approximately 0.003. Using the estimators of σ_ξ^2 and δ_η^2 the approximate variance of the hologram resolution Δx_1 can be expressed as

$$V\left[\Delta x_1\right]_{ss} \cong \left(\frac{\lambda_s}{6}\frac{r_0}{r_1}m_x\right)^2\left\{\frac{\left[r_1^2\, r_0 - r_0(x_1 - m_x\,\bar{\xi})^2\right]^2\,\Delta\xi^2}{\left[r_0(x_1 - m_x\,\bar{\xi}) + r_1(x_1 - x_0)\right]^4}\right.$$

$$\left. + \frac{\left[r_0\,(m_y\,\eta - y_1)\,(x_1 - m_x\,\xi)\right]^2\,\Delta\eta^2}{\left[r_0(x_1 - m_x\,\bar{\xi}) + r_1(x_1 - x_0)\right]^4}\right\} \tag{57}$$

If the holograms are sampled for deviations in scanning receiver positions, then estimates can be calculated using the maximum likelihood method. The estimation of the means $\bar{\xi}$ and $\bar{\eta}$ assuming a normal distribution is

$$\hat{\xi} = \frac{1}{n}\sum_{i=1}^{n}\xi_i = \bar{\xi} \tag{58}$$

$$\hat{\eta} = \frac{1}{n}\sum_{i=1}^{n}\eta_i = \bar{\eta} \tag{59}$$

It is important to note that the estimates of $\bar{\xi}$ and $\bar{\eta}$ have not involved estimates of σ_ξ^2 or σ_η^2. If $\bar{\xi}$ and $\bar{\eta}$ are unknown, then unbiased estimates of σ_ξ^2 and σ_η^2 can be expressed as

$$\hat{\sigma}_\xi^2 = \frac{1}{n-1}\sum_{i=1}^{n}(\xi_i - \bar{\xi})^2 \tag{60}$$

$$\hat{\sigma}_\eta^2 = \frac{1}{n-1}\sum_{i=1}^{n}(\eta_i - \bar{\eta})^2 \tag{61}$$

The variance of Δx_1 can then be expressed as

$$V\left[\Delta x_1\right]_{ss} \cong \left(\frac{\lambda_s\, r_0\, m_x}{2r_1}\right)^2 \left\{ \frac{\left[r_0 r_1^{\,2} - r_0\left(x_1 - \frac{m_x}{n}\sum \xi_i\right)^2\right]^2 (n-1)^{-1} \sum (\xi_i - \bar{\xi})^2}{\left[r_0\left(x_1 - \frac{m_x}{n}\sum \xi_i\right) + r_1(x_1 - x_0)\right]^4} \right.$$

$$\left. + \frac{\left[r_0\left(\frac{m_y}{n}\sum \eta_i - y_1\right)\left(x_1 - \frac{m_x}{n}\sum \xi_i\right)\right] (n-1)^{-1} \sum (\eta_i - \bar{\eta})^2}{\left[r_0\left(x_1 - \frac{m_x}{n}\sum \xi_i\right) + r_1(x_1 - x_0)\right]^4} \right\} \qquad (62)$$

where

$$r_1 = \sqrt{\left(x_1 - \frac{m_x}{n}\sum \xi_i\right)^2 + \left(y_1 - \frac{m_y}{n}\sum \eta_i\right)^2 + z_1^{\,2}} \qquad (63)$$

In order to investigate the effects of position scanning errors on the hologram resolution, we can simplify Eq. (57) in applying the usual valid assumptions in acoustic holography. The maximum aperture dimension is $2x_m$ and the errors are only in the simulated ξ positions of the receiver. The objects are located near the z axis and the hologram to object distances are much greater than the aperture dimensions. The source is located near the z axis. Figure 6 is a simplified diagram of the approximate hologram resolution geometry using these assumptions.

Equation (57) simplifies to the following expression after employing the previously mentioned assumptions and substituting $\bar{\xi} = \xi_m$ for the maximum simulated aperture dimension.

$$V\left[\Delta x_1\right]_{ss} \cong \frac{\lambda_s^2\, z_1^{\,2}\, \Delta\xi^2}{36\, m_x^{\,2}\, \xi_m^{\,4}} \qquad (64)$$

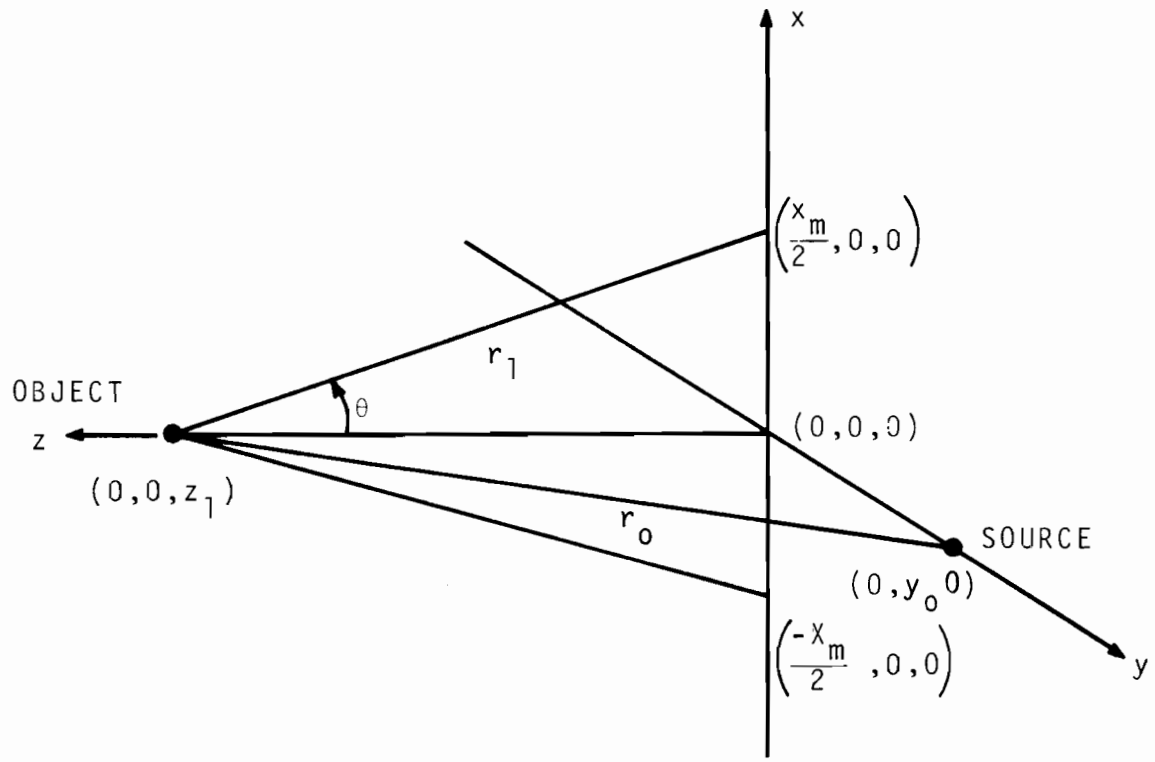

FIGURE 6. Hologram Resolution Geometry

The standard deviation is

$$\sigma\left[\Delta x_1\right]_{ss} \cong \frac{\lambda_s z_1 \Delta\xi}{6 m_x \xi_m^2} \tag{65}$$

The errors in the stationary source hologram resolution vary inversely as the square of the simulated aperture dimension. Theoretically the resolution errors would approach zero if the aperture was infinite. In this case we have an angular aperture approaching π radians and this of course provides infinite resolution. The actual aperture dimension can be related to the simulated dimension by the following equation

$$x_m = m_x \xi_m \tag{66}$$

If we substitute Eq. (66) into Eq. (65), the standard deviation is now a function of the actual scanning aperture dimension x_m.

$$\sigma\left[\Delta x_1\right]_{ss} \cong \frac{\lambda_s z_1 \Delta\xi m_x}{6 x_m^2} \tag{67}$$

Equation (67) shows that demagnification of the hologram increases the resolution errors. Usually the hologram film is demagnified to increase the lateral and radial magnifications. Naturally, if the ratio of the magnifications approach unity, the three dimensional quality of the hologram will be restored.

THE EXPECTED VALUE OF THE STATIONARY SOURCE HOLOGRAM RESOLUTION

The expected value of the hologram resolution is the first term of Eq. (52). The expected value of a constant is the constant itself.

$$E\left[\Delta x_1\right]_{ss} \cong \frac{r_1 r_0 \lambda_s}{2r_0(x_1 - m_x \bar{\xi}) + 2r_1(x_1 - x_0)} \tag{68}$$

If the same assumptions and geometry used to simplify the variance are employed, the expected value of the hologram resolution will simplify to the following expression.

$$E\left[\Delta x_1\right]_{ss} \cong \frac{\lambda_s z_1}{2x_m} \tag{69}$$

The resolution approaches infinity (i.e., $\Delta x_1 \to 0$) when the angular aperture approaches π radians. The resolution is also a function of the object to hologram distance and the wavelength of sound. The resolution of the hologram is dominated by the scanning aperture of the receiver in

the stationary source system, but is also dependent on the scanning source aperture if source scanning is employed.

SIMULTANEOUS SOURCE RECEIVER SCANNING RESOLUTION ERRORS

The stationary source hologram resolution, Eq. (47), can be modified to allow for simultaneous scanning of the source and receiver in the (x-y) plane. If the source and receiver are scanned together, the source position can be defined by the following expressions:

$$x_0 = x + d_1 = m_x \xi + d_1 \tag{70}$$

$$y_0 = y + d_2 = m_y \eta + d_2 \tag{71}$$

The velocities of the source and receiver are related by the following equations.

$$V_0 \alpha = \frac{dx_0}{dt} = \frac{dx}{dt} = Vx \tag{72}$$

$$V_0 \beta = \frac{dy_0}{dt} = \frac{dy}{dt} = Vy \tag{73}$$

Figure 7 is a simplified diagram of the scanning source receiver hologram construction geometry. If we assume the source and receiver occupy the same space, then $d_1 = d_2 = d_3 = 0$.

Substituting Eqs. (70) and (71) into Eq. (47) results in the following expression for the simultaneous source receiver scanned hologram resolution.

$$\Delta x_1(ps) = \frac{\lambda_S \, r_0 r_1}{2(x_1 - m_x \xi)\, r_0 + 2(x_1 - m_x \xi - d_1)\, r_1} \tag{74}$$

where

$$r_0 = \sqrt{(x_1 - m_x \xi - d_1)^2 + (y_1 - m_y \eta - d_2)^2 + (z_1 - z_0)^2}$$

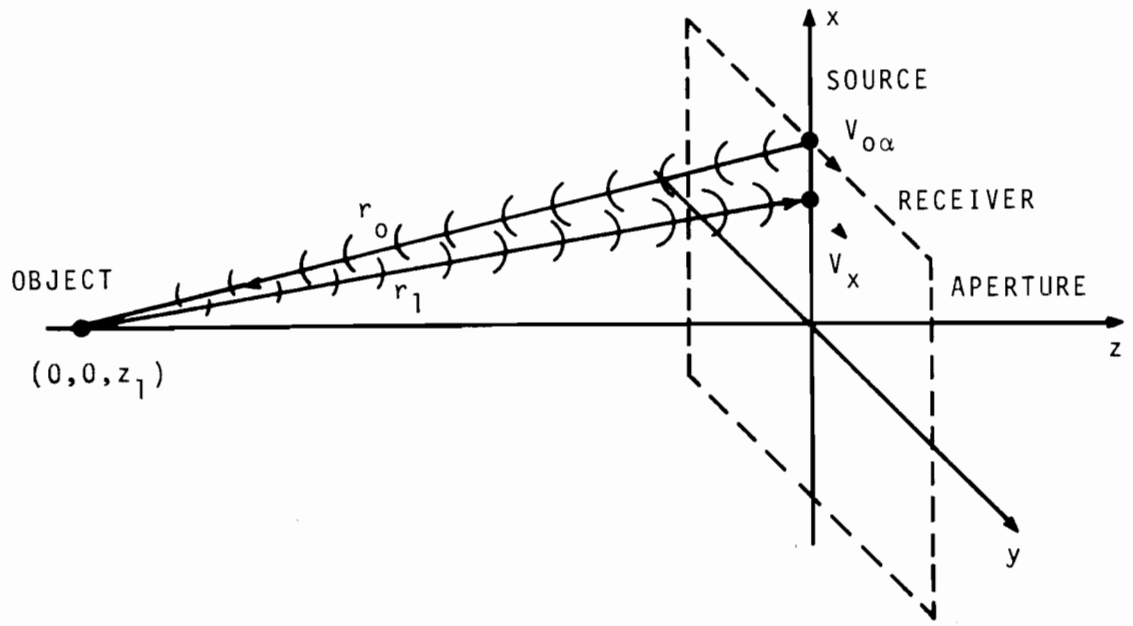

Figure 7. Simultaneous source receiver hologram construction geometry.

and

$$r_1 = \sqrt{(x_1 - m_x\xi)^2 + (y_1 - m_y\eta)^2 + z_1^2} \tag{76}$$

If we assume random position errors in ξ and η, the following statistical models can be used

$$\xi = \bar{\xi} + e_\xi \tag{77}$$

$$\eta = \bar{\eta} + e_\eta \tag{78}$$

where $\bar{\xi}$ and $\bar{\eta}$ are the means. The statistically independent random errors are e_ξ and e_η. It is assumed that $e_\xi \sim N(0,\sigma_\xi^2)$ and $e_\eta \sim N(0,\sigma_\eta^2)$.

We expand Eq. (74) in a Taylor's series about the points $\bar{\xi}$ and $\bar{\eta}$ and retain only the linear terms of ξ and η in the expansion. This

is justified if the errors are small with respect to the measured values of ξ and η (i.e., σ_ξ or $\sigma_\eta < 0.1\ \xi$ or η). The expansion of the resolution is

$$\Delta x_1(ps) = \frac{r_1 r_0\ \lambda_S}{2\left[r_0(x_1 - m_x\overline{\xi}) + r_1(x_1 - m_x\overline{\xi} - d_1)\right]}$$

$$+ m_x\ \lambda_S \frac{r_0(x_1 - m_x\overline{\xi}) + r_1(x_1 - m_x\overline{\xi} - d_1)}{\overline{2}\ \ r_0(x_1 - m_x\overline{\xi}) + r_1(x_1 - m_x\overline{\xi} - d_1)}$$

$$x \frac{\left[r_0 r_1^{-1}(m_x\overline{\xi} - x_1) + r_1 r_0^{-1}(m_x\overline{\xi} - x_1 + d_1)\right]}{\sqrt{2}\left[r_0(x_1 - m_x\overline{\xi}) + r_1(x_1 - m_x\overline{\xi} - d_1)\right]} e_\xi$$

$$- r_1 r_0\ \lambda_S\ m_x \frac{\left[(m_x\overline{\xi} - x_1 + d_1)(x_1 - m_x\overline{\xi})\ r_0^{-1} - (r_0 + r_1)\right]}{2\left[r_0(x_1 - m_x\overline{\xi}) + r_1(x_1 - m_x\overline{\xi} - d_1)\right]^2} e_\xi$$

$$- r_1 r_0\ \lambda_S\ m_x \frac{\left[r_1^{-1}(m_x\overline{\xi} - x_1)(x_1 - m_x\overline{\xi} - d_1)\right]}{2\left[r_0(x_1 - m_x\overline{\xi}) + r_1(x_1 - m_x\overline{\xi} - d_1)\right]^2} e_\xi$$

$$+ \lambda_S\ m_y \frac{\left[r_0(x_1 - m_x\overline{\xi}) + r_1(x_1 - m_x\overline{\xi} - d_1)\right]}{\sqrt{2}\left[r_0(x_1 - m_x\overline{\xi}) + r_1(x_1 - m_x\overline{\xi} - d_1)\right]}$$

$$x \frac{\left[r_1^{-1} r_0(m_y\overline{\eta} - y_1) + r_1 r_0^{-1}(m_y\overline{\eta} + d_2 - y_1)\right]}{\sqrt{2}\left[r_0(x_1 - m_x\overline{\xi}) + r_1(x_1 - m_x\overline{\xi} - d_1)\right]} e_\eta$$

$$- r_1\ \lambda_S\ m_y \frac{\left[(m_y\overline{\eta} + d_2 - y_1)(x_1 - m_x\overline{\xi})\right]}{\sqrt{2}\left[r_0(x_1 - m_x\overline{\xi}) + r_1(x_1 - m_x\overline{\xi} - d_1)\right]^2} e_\eta$$

$$+ r_0\ \lambda_S\ m_y \frac{\left[(y_1 - m_y\overline{\eta})\ (x_1 - m_x\overline{\xi} - d_1)\right]}{2\left[r_0(x_1 - m_x\overline{\xi}) + r_1(x_1 - m_x\overline{\xi} - d_1)\right]^2}\ e_\eta \qquad (79)$$

where

$$r_1 = \sqrt{(m_x\bar{\xi} + d_1 - x_1)^2 + (m_y\bar{\eta} + d_2 - y_1)^2 + (z_1 - z_0)^2} \qquad (80)$$

and

$$r_0 = \sqrt{(x_1 - m_x\bar{\xi})^2 + (y_1 - m_y\bar{\eta})^2 + z_1^2} \quad . \qquad (81)$$

VARIANCE OF THE SIMULTANEOUS SOURCE RECEIVER SCANNED HOLOGRAM RESOLUTION

The approximate variance of the scanning source and receiver hologram resolution is obtained by taking the variance of Eq. (79).

$$V[\Delta x_1(ps)] = \left\{ \lambda_S m_x \frac{\left[r_0(x_1 - m_x\bar{\xi}) + r_1(x_1 - m_x\bar{\xi} - d_1)\right]}{\sqrt{2}\left[r_0(x_1 - m_x\bar{\xi}) + r_1(x_1 - m_x\bar{\xi} - d_1)\right]} \right.$$

$$\times \frac{\left[(m_x\bar{\xi} - x_1)\, r_0 r_1^{-1} + (m_x\bar{\xi} - x_1 + d_1)\, r_1 r_0^{-1}\right]}{\sqrt{2}\left[r_0(x_1 - m_x\bar{\xi}) + r_1(x_1 - m_x\bar{\xi} - d_1)\right]}$$

$$- m_x \lambda_S \frac{\left[(m_x\bar{\xi} - x_1 + d_1)(x_1 - m_x\bar{\xi})\, r_1 - r_0 r_1 (r_0 + r_1)\right]}{2\left[r_0(x_1 - m_x\bar{\xi}) + r_1(x_1 - m_x\bar{\xi} - d_1)\right]^2}$$

$$\left. - m_x \lambda_S r_0 \frac{\left[(m_x\bar{\xi} - x_1)\,(x_1 - m_x\bar{\xi} - d_1)\right]}{2\left[r_0(x_1 - m_x\bar{\xi}) + r_1(x_1 - m_x\bar{\xi} - d_1)\right]^2} \right\}^2 \sigma_\xi^2$$

$$+ \left\{ \lambda_S m_y \frac{\left[r_0(x_1 - m_x\bar{\xi}) + r_1(x_1 - m_x\bar{\xi} - d_1)\right]}{\sqrt{2}\left[r_0(x_1 - m_x\bar{\xi}) + r_1(x_1 - m_x\bar{\xi} - d_1)\right]} \right.$$

$$\times \frac{\left[r_0 r_1^{-1}(m_y\bar{\eta} - y_1) + r_1 r_0^{-1}(m_y\bar{\eta} + d_2 - y_1)\right]}{\sqrt{2}\left[r_0(x_1 - m_x\bar{\xi}) + r_1(x_1 - m_x\bar{\xi} - d_1)\right]}$$

$$- m_x \lambda_S \frac{\left[(m_x\bar{\xi} - x_1 + d_1)(x_1 - m_x\bar{\xi})\, r_1 - r_0 r_1 (r_1 + r_0)\right]}{2\left[r_0(x_1 - m_x\bar{\xi}) + r_1(x_1 - m_x\bar{\xi} - d_1)\right]^2}$$

$$- m_x \lambda_S r_0 \frac{\left[(m_x\bar{\xi} - x_1)(x_1 - m_x\bar{\xi} - d_1)\right]}{2\left[r_0(x_1 - m_x\bar{\xi}) + r_1(x_1 - m_x\bar{\xi} - d_1)\right]^2} \Bigg\}^2 \sigma_\eta^2 \qquad (82)$$

In order to compare the resolution errors of the stationary source configuration with the simultaneous source receiver scanned configuration it is necessary to simplify Eq. (82) by applying the same assumptions as previously done in the stationary source case. The variance of the hologram resolution Eq. (82) simplifies to the following expression if the source and receiver are scanned together (i.e., $r_1 \cong r_0$).

$$V[\Delta x_1(ps)] \cong \frac{\lambda_S^2 z_1^2 \Delta\xi^2}{144 m_x^2 \xi_m^4} \qquad (83)$$

The standard deviation can then be written as

$$\sigma[\Delta x_1(ps)] \cong \frac{\lambda_S z_1 \Delta\xi}{12 m_x \xi_m^2} \qquad (84)$$

where

$$m_x = \frac{x_m}{\xi_m} \qquad (85)$$

This result is very interesting when compared with the stationary source case. The standard deviation of the moving source hologram resolution is identical to the stationary source deviation except for a constant. The stationary source resolution errors are increased by

a factor of two compared with the moving source errors. If we substitute Eq. (85) into the standard deviation, then it is now a function of the actual aperture dimension (i.e., x_m).

$$\sigma[\Delta x_1(ps)] \cong \frac{\lambda_S \, z_1 \, m_x}{12 \, x_m^2} \tag{86}$$

Equation (86) shows that decreasing the aperture and demagnification of the hologram increases the resolution errors.

EXPECTED VALUE OF THE SIMULTANEOUS SOURCE RECEIVER SCANNED HOLOGRAM RESOLUTION

The expected value of the scanning source receiver hologram resolution is obtained by taking the expected value of Eq. (79). The expected value of the resolution is the first term of the expansion.

$$E[\Delta x_1(ps)] = \frac{\lambda_S \, r_0 r_1}{2\left[r_0(x_1 - m_x\bar{\xi}) + r_1(x_1 - m_x\bar{\xi} - d_1)\right]} \tag{87}$$

If we use the same conditions, as previously applied to simplify the variance, then Eq. (87) can be reduced to the following expression.

$$E[\Delta x_1(ps)] \cong \frac{\lambda_S \, z_1}{4 \, m_x \, \xi_m} \tag{88}$$

where $r_1 \approx r_0$, and $\bar{\xi} = \xi_m$.

Equation (88) can be expressed in terms of the actual scanning aperture dimension as previously done.

$$E[\Delta x_1(ps)] \cong \frac{\lambda_S \, z_1}{4 \, x_m} \tag{89}$$

This result shows that the resolution is increased by source scanning. In this particular example where the source and receiver are at the same position, the system provides twice the resolution of a stationary source system. The errors are also decreased by scanning a point source with the receiver. The ratio of the stationary and moving source standard deviations reduces to the following approximation.

$$\frac{\sigma[\Delta x_1(ss)]}{\sigma[\Delta x_1(ps)]} = 2 \tag{90}$$

The ratio shows that by scanning a point source with the receiver decreases the hologram resolution errors by a factor of two.

V. RADIAL MAGNIFICATION ERRORS IN ACOUSTIC SCANNED HOLOGRAPHY

HOLOGRAM RADIAL MAGNIFICATION

The hologram radial magnification is defined as the partial derivative of the image point (r_b) with respect to the object point distance (r_1). The radial magnification can be expressed mathematically as

$$M_R = \frac{\partial r_b}{\partial r_1} \quad . \tag{91}$$

The image location equations (employing parallel source receiver motion) relating image and object point distances are (see Appendix C)

$$\frac{1}{r_b} = \pm \frac{\lambda_L}{\lambda_S} \left(\frac{V_x}{V_\xi}\right)^2 \left[\frac{1}{r_1} + \left(\frac{V_{o\alpha}}{V_x}\right)^2 \frac{1}{r_0} - \frac{1}{r_2}\right] - \frac{1}{r_a} \quad , \tag{92}$$

$$\frac{1}{r_b} = \pm \frac{\lambda_L}{\lambda_S} \left(\frac{V_y}{V_\eta}\right)^2 \left[\frac{1}{r_1} + \left(\frac{V_{o\beta}}{V_y}\right)^2 \frac{1}{r_0} - \frac{1}{r_2}\right] - \frac{1}{r_a} \quad , \tag{93}$$

where the plus and minus signs refer to the conjugate and the true images, respectively.

Differentiating Eqs. (92) and (93) with respect to r_b and r_1 the radial magnification can be expressed as

$$M_R(V_\xi) = \pm \frac{\lambda_L}{\lambda_S} \left(\frac{r_b}{r_1}\right)^2 \left[\left(\frac{V_x}{V_\xi}\right)^2 + \left(\frac{V_{o\alpha}}{V_\xi}\right)^2\right] \quad , \tag{94}$$

$$M_R(V_\eta) = \pm \frac{\lambda_L}{\lambda_S} \left(\frac{r_b}{r_1}\right)^2 \left[\left(\frac{V_y}{V_\eta}\right)^2 + \left(\frac{V_{o\beta}}{V_\eta}\right)^2\right] \quad . \tag{95}$$

If the radial magnification is to be undistorted, then the following conditions on the actual and simulated scanning velocities must be satisfied:

$$\left(\frac{V_x}{V_\xi}\right)^2 + \left(\frac{V_{o\alpha}}{V_\xi}\right)^2 = \left(\frac{V_y}{V_\eta}\right)^2 + \left(\frac{V_{o\beta}}{V_\eta}\right)^2 \quad . \tag{96}$$

If the source receiver motion is identical, then $V_{o\xi} = V_x$, $V_{o\eta} = V_y$ and the conditions of Eq. (96) reduce to the following expression:

$$\frac{V_x}{V_\xi} = \frac{V_y}{V_\eta} \quad . \tag{97}$$

After substitution of Eq. (97) into Eqs. (94) and (95), the radial hologram magnification for simultaneous source receiver scanning is defined by the following equations:

$$M_R(V_\xi)ps \cong \pm 2\,\frac{\lambda_L}{\lambda_S}\left(\frac{r_b}{r_1}\frac{V_x}{V_\xi}\right)^2 \quad , \tag{98}$$

$$M_R(V_\eta)ps \cong \pm 2\,\frac{\lambda_L}{\lambda_S}\left(\frac{r_b}{r_1}\frac{V_y}{V_\eta}\right)^2 \quad . \tag{99}$$

If the source is stationary (i.e., $V_{o\alpha} = V_{o\beta} = 0$), then the radial hologram magnification is increased approximately by a factor of two. This implies that scanning the source decreases the radial magnification of the hologram. The radial magnification employing a fixed source of illumination (or constant phase across the aperture) is given by the following expressions:

$$M_R(V_\xi)ss = \pm\,\frac{\lambda_L}{\lambda_S}\left(\frac{\overline{r_b}}{r_1}\frac{V_x}{V_\xi}\right)^2 \quad , \tag{100}$$

$$M_R(V_\eta)ss = \pm \frac{\lambda_L}{\lambda_S}\left(\frac{\overline{r}_b}{r_1}\frac{V_y}{V_\eta}\right)^2 \quad . \tag{101}$$

VARIANCE OF THE RADIAL HOLOGRAM MAGNIFICATION

To derive the variance and the expected value of the radial magnification, we assume the following linear statistical models for the simulated velocities V_ξ and V_η:

$$V_\xi = \overline{V}_\xi + e_{V\xi} \quad , \tag{102}$$

$$V_\eta = \overline{V}_\eta + e_{V\eta} \quad . \tag{103}$$

The simulated velocities V_ξ and V_η are assumed to be statistically independent random variables with their respective means $\overline{V}_\xi$, $\overline{V}_\eta$ and variances $\sigma_{V_\xi}^2$, $\sigma_{V_\eta}^2$. The velocity errors e_{V_ξ} and e_{V_η} are assumed to be independent and normally distributed with zero means:

$$e_{V_\xi} \sim N\left(0, \sigma_{V_\xi}^2\right) \quad , \tag{104}$$

$$e_{V_\eta} \sim N\left(0, \sigma_{V_\eta}^2\right) \quad . \tag{105}$$

If the errors e_{V_ξ} and e_{V_η} are small with respect to the measured values of the independent variables (V_ξ and V_η), then the radial magnification can be expanded in a Taylor's series with retention of only the linear terms. (See Appendices A and B.) After a Taylor's expansion of Eqs. (98) and (99) about their respective mean values $\overline{V}_\xi$, $\overline{V}_\eta$ and neglecting terms of degree higher than in the first deviations $(V_\xi - \overline{V}_\eta)$ and $(V_\xi - \overline{V}_\eta)$, we have the following expressions:

$$M_R(V_\xi)ps \cong \pm \left\{ 2\frac{\lambda_L}{\lambda_S}\left(\frac{r_b}{r_1}\frac{V_x}{\overline{V}_\xi}\right)^2 - 4\ \frac{\lambda_L}{\lambda_S}\left(\frac{r_b}{r_1}\frac{V_x}{\overline{V}_\xi}\right)^2 \frac{(V_\xi - \overline{V}_\xi)}{\overline{V}_\xi} \right\}, \quad (106)$$

$$M_R(V_\eta)ps \cong \pm \left\{ 2\frac{\lambda_L}{\lambda_S}\left(\frac{r_b}{r_1}\frac{V_y}{\overline{V}_\eta}\right)^2 - 4\frac{\lambda_L}{\lambda_S}\left(\frac{r_b}{r_1}\frac{V_y}{\overline{V}_\eta}\right)^2 \frac{(V_\eta - \overline{V}_\eta)}{\overline{V}_\eta} \right\}. \quad (107)$$

The variances of the hologram radial magnifications with respect to their corresponding velocity errors e_{V_ξ} and e_{V_η} are given by the following equations:

$$V\left[M_R(V_\xi)ps\right] = 16\left(\frac{\lambda_L}{\lambda_S}\right)^2 \left[\frac{r_b}{r_1}\frac{V_x}{\overline{V}_\xi}\right]^4 \frac{\sigma_{V_\xi}^2}{\overline{V}_\xi^2}, \quad (108)$$

$$V\left[M_R(V_\eta)ps\right] = 16\left(\frac{\lambda_L}{\lambda_S}\right)^2 \left[\frac{r_b}{r_1}\frac{V_y}{\overline{V}_\eta}\right]^4 \frac{\sigma_{V_\eta}^2}{\overline{V}_\eta^2}. \quad (109)$$

The variance of the stationary source radial magnification is greater than the simultaneous source receiver motion variance. The corresponding standard deviations for the radial hologram magnification are given by:

$$\sigma M_R(V_\xi)ps = 4\ \frac{\lambda_L}{\lambda_S}\left(\frac{r_b}{r_1}\frac{V_x}{\overline{V}_\xi}\right)^2 \frac{\sigma_{V_\xi}}{\overline{V}_\xi}, \quad (110)$$

$$\sigma M_R(V_\eta)ps = 4\ \frac{\lambda_L}{\lambda_S}\left(\frac{r_b}{r_1}\frac{V_y}{\overline{V}_\eta}\right)^2 \frac{\sigma_{V_\eta}}{\overline{V}_\eta}. \quad (111)$$

The radial magnifications $M_R(V_\xi)ps$ and $M_R(V_\eta)ps$ are linear functions of the random variables V_ξ and V_η. The radial magnifications can be expressed as

$$M_R(V_\xi)ps \cong a + b\ (V_\xi - \overline{V}_\xi) \quad (112)$$

and

$$M_R(V_\eta)ps \cong c + d\ (V_\eta - \overline{V}_\eta) \tag{113}$$

where a, b, c and d are constants.

The variance of the sum of the radial magnifications $M_R(V_\xi)ps$ and $M_R(V_\eta)ps$ is

$$V\left[M_R(V_\xi)ps + M_R(V_\eta)ps\right] = b^2\ V\left[e_{V_\xi}\right] + d^2\ V\left[e_{V_\eta}\right] + 2\ bd\ \mathrm{cov}\left[e_{V_\xi}, e_{V_\eta}\right] \tag{114}$$

where covariance is zero.

The final expression for Eq. (114) is given by the following expression:

$$V\left[M_R(V_\xi)ps + M_R(V_\eta)ps\right] = 16\left(\frac{\lambda_L}{\lambda_S}\right)^2\left(\frac{r_b}{r_1}\right)^4\left\{\left(\frac{V_x}{\overline{V}_\xi}\right)^2 \frac{\sigma_{V_\xi}^{\ 2}}{\overline{V}_\xi^{\ 2}} + \left(\frac{V_y}{\overline{V}_\eta}\right)^4 \frac{\sigma_{V_\eta}}{\overline{V}_\eta^{\ 2}}\right\} \quad . \tag{115}$$

Estimates of σ_{V_ξ} and σ_{V_η} can be made if the expected deviations $(V_\xi - \overline{V}_\xi)$, $(V_\eta - \overline{V}_\eta)$ of the simulated velocities are assumed not to exceed three standard deviations. The estimators of σ_{V_ξ} and σ_{V_η} are given by the following expressions:

$$\hat{\sigma}_{V_\xi} = \frac{\Delta V_\xi}{3} \quad , \tag{116}$$

$$\hat{\sigma}_{V_\eta} = \frac{\Delta V_\eta}{3} \quad . \tag{117}$$

If three sigma value is assumed, then the probability of the velocity deviations exceeding ΔV_ξ, ΔV_η is 0.0027. Equation (115) can then be expressed as

$$V\left[M_R(V_\xi)ps + M_R(V_\eta)ps\right] = \frac{16}{9}\left(\frac{\lambda_L}{\lambda_S}\right)^2\left(\frac{\bar{r}_b}{r_1}\right)^4\left\{\left(\frac{V_x}{\bar{V}_\xi}\right)^4 \frac{\Delta V_\xi^{\,2}}{\bar{V}_\xi^{\,2}} + \left(\frac{V_y}{\bar{V}_\eta}\right)^2 \frac{\Delta V_\eta^{\,2}}{\bar{V}_\eta^{\,2}}\right\} \quad . \tag{118}$$

If we assume the expected deviations in the simulated velocities ratios $\frac{\Delta V_\xi}{\bar{V}_\xi}$ and $\frac{\Delta V_\eta}{\bar{V}_\eta}$ are approximately equal and imposing the stigmatic condition $\frac{V_x}{\bar{V}_\xi} = \frac{V_y}{\bar{V}_\eta}$, then Eq. (118) reduces to the following expression:

$$V\left[M_R(V_\xi)ps + M_R(V_\eta)ps\right] = \frac{32}{9}\left(\frac{\lambda_L}{\lambda_S}\right)^2\left(\frac{\bar{r}_b}{r_1}\frac{V_x}{\bar{V}_\xi}\right)^4 \frac{V_\xi^{\,2}}{\bar{V}_\xi^{\,2}} \quad . \tag{119}$$

The standard deviation of the radial hologram magnification is

$$\sigma M_R(ps) = \frac{4\sqrt{2}}{3}\,\frac{\lambda_L}{\lambda_S}\left(\frac{\bar{r}_b}{r_1}\,\frac{V_x}{\bar{V}_\xi}\right)^2 \frac{\Delta V_\xi}{\bar{V}_\xi} \quad . \tag{120}$$

The hologram aperture dimension L_x can be defined as $L_x = V_x T$ and the simulated aperture as $L_\xi = V_\xi T$, where T is the hologram line scanning time. The ratio of the velocities is then defined in terms of the aperture dimensions

$$\frac{V_x}{V_\xi} = \frac{L_x}{L_\xi} \quad . \tag{121}$$

The standard deviation can now be related to the aperture dimensions. The radial magnification error increases

$$\sigma M_R(ps) = \frac{4\sqrt{2}}{3} \frac{\lambda_L}{\lambda_S} \left(\frac{r_b}{r_1}\right)^2 \left(\frac{L_x}{L_\xi}\right)^2 \frac{\Delta V_\xi}{\overline{V}_\xi} \tag{122}$$

as the square of the actual to simulated aperture dimensions. Usually the simulated aperture is much smaller than the actual aperture scanned by the source and receiver. Equation (122) shows that reducing the simulated aperture dimension by a factor of four increases the radial magnification error by a factor of sixteen. The standard deviation also varies directly as the simulated velocity deviations (ΔV_ξ) or (ΔV_η).

EXPECTED VALUE OF THE RADIAL HOLOGRAM MAGNIFICATION

The expected or mean value of the radial magnification for simultaneous source receiver scanning is given by the following expressions.

$$E[M_R(V_\xi)ps] \cong \pm 2 \frac{\lambda_L}{\lambda_S} \left(\frac{r_b}{r_1} \frac{V_x}{\overline{V}_\xi}\right)^2 , \tag{123}$$

$$E[M_R(V_\eta)ps] \cong \pm 2 \frac{\lambda_L}{\lambda_S} \left(\frac{r_b}{r_1} \frac{V_y}{\overline{V}_\eta}\right)^2 , \tag{124}$$

where V_ξ and V_η are the average values of the simulated scanning velocities. The expected value of the stationary source radial magnification is decreased by a factor of two from the simultaneous source receiver radial magnification.

To avoid radial magnification distortion the expected values, Eqs. (123) and (124), must be equal. This implies the identical restrictions as mentioned previously, the velocity ratios must remain

equal. The expected value of the sum of the radial magnifications $M_R(V_\xi)ps$ and $M_R(V_\eta)ps$ can be written as

$$E\left[a + b\, e_{V_\xi} + c + d\, e_{V_\eta}\right] = a + b \tag{125}$$

where

$$a = \pm\, 2\frac{\lambda_L}{\lambda_S}\left(\frac{r_b}{r_1}\frac{V_x}{\overline{V}_\xi}\right)^2 \tag{126}$$

and

$$b = \pm\, 2\frac{\lambda_L}{\lambda_S}\left(\frac{r_b}{r_1}\frac{V_y}{\overline{V}_\eta}\right)^2 \quad . \tag{127}$$

Equation (125) can be written in the following form:

$$E\left[M_R(V_\xi)ps + M_R(V_\eta)ps\right] = \pm\, 2\frac{\lambda_L}{\lambda_S}\left(\frac{r_b}{r_1}\right)^2\left[\left(\frac{V_x}{\overline{V}_\xi}\right)^2 + \left(\frac{V_y}{\overline{V}_\eta}\right)^2\right] \quad .$$

The expected values of the radial magnifications can be expressed in terms of the actual and simulated aperture dimensions:

$$E\left[M_R(V_\xi)_{ps}\right] = \pm\, 2\frac{\lambda_L}{\lambda_S}\left(\frac{r_b}{r_1}\frac{L_x}{L_\xi}\right)^2 \quad , \tag{128}$$

$$E\left[M_R(V_\eta)ps\right] = \pm\, 2\frac{\lambda_L}{\lambda_S}\left(\frac{r_b}{r_1}\frac{L_x}{L_\eta}\right)^2 \quad . \tag{129}$$

Equations (128) and (129) show that decreasing the simulated aperture dimensions L_ξ and L_η with respect to the actual aperture (i.e., demagnification of the hologram) increases the radial magnification.

VI. LATERAL MAGNIFICATION ERRORS IN ACOUSTIC SCANNED HOLOGRAPHY

HOLOGRAM LATERAL MAGNIFICATION

The hologram lateral magnification as defined by Hildebrand [12] is the partial derivative of the image point distance with respect to the object to hologram distance. The lateral magnification can then be expressed mathematically by the following equation:

$$M_L(x) = \frac{\partial x_b}{\partial x_1} \quad , \tag{130}$$

$$M_L(y) = \frac{\partial y_b}{\partial y_1} \quad . \tag{131}$$

This is the magnification in the (x,y) plane of the object space (see Fig. 5). The image location equations for source receiver scanning relating x_b, y_b and x_1, y_1 are given by the following equations (see Appendix C):

$$\frac{x_b}{r_b} = \pm \frac{\lambda_L}{\lambda_S} \frac{V_x}{V_\xi} \left[\frac{x_1}{r_1} + \frac{(x_1 - x_0)}{r_1} - \frac{x_2}{r_2} \right] - \frac{x_a}{r_a} \quad , \tag{132}$$

$$\frac{y_b}{r_b} = \pm \frac{\lambda_L}{\lambda_S} \frac{V_y}{V_\eta} \left[\frac{y_1}{r_1} + \frac{(y_1 - y_0)}{r_1} - \frac{y_2}{r_2} \right] - \frac{y_a}{r_a} \tag{133}$$

where $r_0 = r_1$, $V_{o\alpha} = V_x$ and $V_{o\beta} = V_y$. The plus and minus signs refer to the conjugate and true images, respectively.

Differentiating Eqs. (132) and (133) with respect to x_b, y_b, x_1, and y_1, the lateral hologram magnification is given by the following equations:

$$M_L(x)ps = \pm 2 \frac{\lambda_L}{\lambda_S} \frac{V_x}{V_\xi} \frac{r_b}{r_1} \quad , \tag{134}$$

$$M_L(V_\eta)ps = \pm 2 \frac{\lambda_L}{\lambda_S} \frac{V_y}{V_\eta} \frac{r_b}{r_1} \quad . \tag{135}$$

If the source is stationary, then Eqs. (134) and (135) reduce to the following expressions:

$$M_L(x) = \pm \frac{\lambda_L}{\lambda_S} \frac{V_x}{V_\xi} \frac{\overline{r}_b}{r_1} \quad , \tag{136}$$

$$M_L(y) = \pm \frac{\lambda_L}{\lambda_S} \frac{V_y}{V_\eta} \frac{\overline{r}_b}{r_1} \quad . \tag{137}$$

VARIANCE OF THE LATERAL HOLOGRAM MAGNIFICATION

The same conditions that were assumed in deriving the variance and expected value of the radial magnification were used in obtaining the variance and expected value in the lateral hologram magnification. After a Taylor's series expansion of Eqs. (134) and (135) about their rexpective mean values $\overline{V}_\xi$, $\overline{V}_\eta$ and retaining only the linear terms of the expansion we have the following expressions

$$M_L(x)ps = \pm 2 \frac{\lambda_L}{\lambda_S} \frac{V_x}{\overline{V}_\xi} \frac{r_b}{r_1} \mp 2 \frac{\lambda_L}{\lambda_S} \frac{V_x}{\overline{V}_\xi^2} \frac{r_b}{r_1} (V_\xi - \overline{V}_\xi) \quad , \tag{138}$$

$$M_L(y)ps = \pm 2 \frac{\lambda_L}{\lambda_S} \frac{V_y}{\overline{V}_\eta} \frac{r_b}{r_1} \mp 2 \frac{\lambda_L}{\lambda_S} \frac{V_y}{\overline{V}_\eta^2} \frac{r_b}{r_1} (V_\eta - \overline{V}_\eta) \quad . \tag{139}$$

The variances of the hologram lateral magnifications with respect to their corresponding errors e_{V_ξ} and e_{V_η} are given by the following equations:

$$V\left[M_L(x)ps\right] = 4\left[\frac{\lambda_L}{\lambda_S}\frac{V_x}{\overline{V}_\xi}\frac{r_b}{r_1}\right]^2 \frac{\sigma_{V_\xi}^2}{\overline{V}_\xi^2} \quad , \tag{140}$$

$$V\left[(M_L(y)ps\right] = 4\left[\frac{\lambda_L}{\lambda_S}\frac{V_y}{\overline{V}_\eta}\frac{r_b}{r_1}\right]^2 \frac{\sigma_{V_\eta}^2}{\overline{V}_\eta^2} \quad . \tag{141}$$

The variance of the stationary source lateral magnification is approximately equal to the simultaneous source receiver motion variance. The corresponding standard deviations for the lateral hologram magnification are given by:

$$\sigma M_L(x)ps = 2\frac{\lambda_L}{\lambda_S}\frac{V_x}{\overline{V}_\xi}\frac{r_b}{r_1}\frac{\sigma_{V_\xi}}{\overline{V}_\xi} \quad , \tag{142}$$

$$\sigma M_L(x)ps = 2\frac{\lambda_L}{\lambda_S}\frac{V_y}{\overline{V}}\frac{r_b}{r_1}\frac{\sigma_{V_\eta}}{\overline{V}_\eta} \quad . \tag{143}$$

The variance of the sum of the lateral magnifications $M_L(x)ps$ and $M_L(y)ps$ is

$$V\left[M_L(x)ps + M_L(y)ps\right] = 4\left(\frac{\lambda_L}{\lambda_S}\frac{r_b}{r_1}\right)^2\left\{\left(\frac{V_x}{\overline{V}_\xi}\right)^2\frac{\sigma_{V_\xi}^2}{\overline{V}_\xi^2} + \left(\frac{V_y}{\overline{V}_\eta}\right)^2\frac{\sigma_{V_\eta}^2}{\overline{V}_\eta^2}\right\} \quad . \tag{144}$$

The estimators of σ_{V_ξ} and σ_{V_η} are given by the following expressions:

$$\hat{\sigma}_{V_\xi} = \frac{\Delta V_\xi}{3} \quad , \tag{145}$$

$$\hat{\sigma}_{V_\eta} = \frac{\Delta V_\eta}{3} \quad . \tag{146}$$

This assumes the deviations will never exceed the three sigma values. Equation (144) can be expressed in terms of the estimators:

$$V\left[M_L(x)ps + M_L(y)ps\right] = \frac{4}{9}\left(\frac{\lambda_L}{\lambda_S}\frac{r_b}{r_1}\right)^2\left\{\left(\frac{V_x}{\overline{V}_\xi}\right)^2\frac{\Delta V_\xi^{\,2}}{\overline{V}_\xi^{\,2}} + \left(\frac{V_y}{\overline{V}_\eta}\right)^2\frac{\Delta V_\eta^{\,2}}{\overline{V}_\eta^{\,2}}\right\} \quad . \tag{147}$$

If we assume the expected deviations in the simulated velocities ratios to be approximately equal and impose the stigmatic conditions, then Eq. (147) reduces to the following expression:

$$V\left[M_L(x)ps + M_L(y)ps\right] = \frac{8}{9}\left[\frac{\lambda_L}{\lambda_S}\frac{r_b}{r_1}\frac{V_x}{\overline{V}_\xi}\frac{\Delta V_\xi}{\overline{V}_\xi}\right]^2 \quad . \tag{148}$$

The standard deviation of the lateral hologram magnification reduces to

$$\sigma M_L(ps) = \frac{4\sqrt{2}}{3}\frac{\lambda_L}{\lambda_S}\frac{r_b}{r_1}\left(\frac{L_x}{L_\xi}\right)\frac{\Delta V_\xi}{\overline{V}_\xi} \tag{149}$$

where the ratio of the velocities has been defined in terms of the actual and simulated apertures (i.e., $V_x/V_\xi = L_x/L_\xi$

$$V_x/V_\xi = L_x/L_\xi\Big) \quad . \tag{150}$$

The lateral magnification error increases directly as the ratio of the actual to simulated aperture dimension and the deviation in the simulated velocities ΔV_ξ or ΔV_η.

EXPECTED VALUE OF THE LATERAL HOLOGRAM MAGNIFICATION

The expected value of the lateral magnification for simultaneous source receiver scanning is given by the following expressions:

$$E\left[M_L(x)ps\right] = \pm\ 2\frac{\lambda_L}{\lambda_S}\frac{V_x}{\overline{V}_\xi}\frac{r_b}{r_1} \quad , \tag{151}$$

$$E\left[M_L(y)ps\right] = \pm\ 2\frac{\lambda_L}{\lambda_S}\frac{V_y}{\overline{V}_\eta}\frac{r_b}{r_1} \tag{152}$$

where the (+) and (-) signs refer to the conjugate and true images, respectively.

The expected value of the lateral hologram magnification can be expressed in terms of the actual and simulated aperture dimensions:

$$E\left[M_L(x)ps\right] = \pm\ 2\frac{\lambda_L}{\lambda_S}\frac{L_x}{L_\xi}\frac{r_b}{r_1} \quad , \tag{153}$$

$$E\left[M_L(y)ps\right] = \pm\ 2\frac{\lambda_L}{\lambda_S}\frac{L_y}{L_\eta}\frac{r_b}{r_1} \quad . \tag{154}$$

The result is similar to the radial magnification example, the lateral magnification is identical if the source is not scanned. The same conditions must be employed to eliminate lateral magnification distortion also (i.e., $\frac{V_x}{V_\xi} = \frac{V_y}{V_\eta}$).

To avoid distortion in the hologram magnification, the radial magnification must equal the lateral magnification. In acoustic holography the sound to light wavelength ratio is usually much greater than one and this factor alone introduces magnification distortion in the hologram. The radial image distances are magnified or stretched

many times more than the lateral image distances. If the recording acoustic wavelength in water corresponds to a frequency of 1 MHz and the reconstructing wavelength is 6328 Å, the image will be elongated approximately 2500 times. Equations (155) and (156) are the ratios of the radial and lateral magnifications, if the reference and reconstruction sources are plane waves (i.e., $r_2 = r_a \to \infty$):

$$\frac{M_R(x)ps}{M_L(x)ps} = \frac{1}{2}\frac{\lambda_S}{\lambda_L}\frac{L_\xi}{L_x} \quad , \tag{155}$$

$$\frac{M_R(y)ps}{M_L(y)ps} = \frac{1}{2}\frac{\lambda_S}{\lambda_L}\frac{L_\eta}{L_y} \quad . \tag{156}$$

If the illuminating source is stationary, the ratios are increased by a factor of two:

$$\frac{M_R(x)ss}{M_L(x)ss} = \frac{\lambda_S}{\lambda_L}\frac{L_\xi}{L_x} \quad , \tag{157}$$

$$\frac{M_R(y)ss}{M_L(y)ss} = \frac{\lambda_S}{\lambda_L}\frac{L_\eta}{L_y} \quad . \tag{158}$$

Equations (155), (156), (157) and (158) show it is theoretically possible to obtain equal magnifications by requiring the ratios to be unity.

The hologram magnification distortion can be eliminated in two ways: 1) construct and reconstruct the hologram with the same wavelength (e.g., optical hologram using the same laser to construct and

reconstruct the hologram, 2) require the simulated to actual aperture dimension ratio to equal the light to sound wavelength ratio in the stationary source case.

$$\frac{L_\xi}{L_x} = \frac{L_\eta}{L_y} = \frac{\lambda_L}{\lambda_S} \quad . \tag{159}$$

This is a very impractical requirement for small apertures because the simulated aperture or hologram film would have to be demagnified 2500 times if the construction source was 1 MHz sound in water and the reconstruction source a helium-neon laser. Typical actual scanning apertures in the laboratory are approximately 10 cm square and the hologram would have to be reduced to 4×10^{-3} cm. If large scanning apertures are employed, then magnification distortion in acoustic holography could be eliminated. Using 10 MHz sound in water and helium-neon laser for reconstruction, the actual aperture size (for a 3 cm x 3 cm hologram) would be 100 meter x 100 meters. It appears that magnification distortion in acoustic holography will always be present and this results in apparent loss of the three-dimensional effect that is so characteristic of optical holograms. The radial distortion in the acoustic hologram obscures the depth information and the images appear two-dimensional. The information is there and can be viewed by focusing on different planes in depth parallel to the hologram plane.

VII. IMAGE POSITION ERRORS AS A RESULT OF RANDOM VELOCITY ERRORS IN THE ACOUSTIC SCANNING RECEIVER

The image point distance r_b is defined in terms of the wavelength, velocity ratios and geometrical distances (r_1, r_2, and r_a). The distances r_1, r_2 and r_a are constant as required in the derivation of the image location equations. The acoustic wavelength λ_S and the light wavelength λ_L are constant during the hologram construction and reconstruction. The horizontal and vertical components of the simulated scanning receiver velocity are assumed to contain random errors. The image location distance is given by the following expressions:

$$r_b(V_\xi)ps = \pm \frac{\lambda_S}{\lambda_L}\left(\frac{V_\xi}{V_x}\right)^2\left[\frac{r_a r_1 r_2}{r_a(2r_2 - r_1) \mp r_1 r_2 \frac{\lambda_S}{\lambda_L}\left(\frac{V_\xi}{V_y}\right)^2}\right], \qquad (160)$$

$$r_b(V_\eta)ps = \pm \frac{\lambda_S}{\lambda_L}\left(\frac{V_\eta}{V_y}\right)^2\left[\frac{r_a r_1 r_2}{r_a(2r_2 - r_1) \mp r_1 r_2 \frac{\lambda_S}{\lambda_L}\left(\frac{V_\eta}{V_y}\right)^2}\right] \qquad (161)$$

where the source and receiver are scanned; the upper and lower signs refer to the conjugate and true images, respectively.

Equations (160) and (161) are required to remain equal to prevent astigmatism in the hologram. This condition requires the velocity ratio to be equal.

If we assume the following linear statistical models for the simulated velocities:

$$V_\xi = \overline{V}_\xi + e_{V_\xi} \quad , \tag{162}$$

$$V_\eta + \overline{V}_\eta + e_{V_\eta} \quad , \tag{163}$$

where V_ξ and V_η are statistically independent random variables with their respective mean values $\overline{V}_\xi$, $\overline{V}_\eta$ and variances $\sigma_{V_\xi}^2$, $\sigma_{V_\eta}^2$. The random errors e_{V_ξ} and e_{V_η} are assumed to be normally distributed with zero means:

$$e_{V_\xi} \sim N\left(0, \sigma_{V_\xi}^2\right) \quad , \tag{164}$$

$$e_{V_\eta} \sim N\left(0, \sigma_{V_\eta}^2\right) \quad . \tag{165}$$

We expand the function $r_b(V_\xi)$ps and $r_b(V_\eta)$ps in Taylor's series about their respective means $\overline{V}_\xi$, $\overline{V}_\eta$ and retain only the linear terms in the expansion:

$$r_b(V)ps \cong \pm \frac{\lambda_S}{\lambda_L} \left\{ \left(\frac{\overline{V}_\xi}{V_x}\right)^2 \left[\frac{r_a r_1 r_2}{r_a(2r_2 - r_1) \mp r_1 r_2 \frac{\lambda_S}{\lambda_L}\left(\frac{\overline{V}_\xi}{V_x}\right)^2} \right] \right.$$

$$\left. + \frac{2}{V_x^2} \frac{r_a^2 r_1 r_2 (2r_2 - r_1) \overline{V}_\xi e_{V_\xi}}{\left[r_a(2r_2 - r_1) \mp r_1 r_2 \frac{\lambda_S}{\lambda_L}\left(\frac{\overline{V}_\xi}{V_x}\right)^2 \right]^2} \right\} , \tag{166}$$

$$r_b(V_\eta)ps \cong \pm \frac{\lambda_S}{\lambda_L}\left\{\left(\frac{\overline{V}_\eta}{\overline{V}_y}\right)^2\left[\frac{r_a r_1 r_2}{r_a(2r_2 - r_1) \mp r_1 r_2 \frac{\lambda_S}{\lambda_L}\left(\frac{\overline{V}_\eta}{\overline{V}_y}\right)^2}\right]\right.$$

$$\left. + \frac{2}{V_y^2}\frac{r_a^2 r_1 r_2 (2r_2 - r_1)\overline{V}_\eta e_{V_\eta}}{\left[r_a(2r_2 - r_1) \mp r_1 r_2 \frac{\lambda_S}{\lambda_L}\left(\frac{\overline{V}_\eta}{\overline{V}_y}\right)^2\right]^2}\right\} . \qquad (167)$$

VARIANCE OF THE IMAGE POINT POSITION

The variances of the image position distance r_b with respect to the corresponding velocity errors e_{V_ξ} and e_{V_η} are given by the following expressions:

$$V\left[r_b(V_\xi)ps\right] \cong \left(\frac{2\lambda_S}{V_x^2 \lambda_L}\right)^2\left\{\frac{r_a^2 r_1 r_2 (2r_2 - r_1)\overline{V}_\xi}{\left[r_a(2r_2 - r_1) \mp r_1 r_2 \frac{\lambda_S}{\lambda_L}\left(\frac{\overline{V}_\xi}{\overline{V}_x}\right)^2\right]^2}\right\}^2 \sigma_{V_\xi}^2 , \qquad (168)$$

$$V\left[r_b(V_\eta)ps\right] \cong \left(\frac{2\lambda_S}{V_y^2 \lambda_L}\right)^2\left\{\frac{r_a^2 r_1 r_2 (2r_2 - r_1)\overline{V}_\eta}{\left[r_a(2r_2 - r_1) \mp r_1 r_2 \frac{\lambda_S}{\lambda_L}\left(\frac{\overline{V}_\eta}{\overline{V}_y}\right)^2\right]^2}\right\}^2 \sigma_{V_\eta}^2 . \qquad (169)$$

The variance of the sum of the image point positions $r_b(V_\xi)ps$ and $r_b(V_\eta)ps$ is the sum of the variances if the random variables are independent. The simulated velocities V_ξ and V_η are assumed to be independent random variables and this implies that the covariance is zero. The variance of the image position for a stationary source hologram is decreased by a factor of four from the source receiver scanning case.

The variance of the sum is given by the following expression:

$$V\left[r_b(V_\xi)ps + r_b(V_\eta)ps\right] \cong 4\left(\frac{\lambda_S}{\lambda_L}\right)^2 \frac{r_a^4\, r_1^2\, r_2^2(2r_2 - r_1)^2\, \overline{V}_\xi^2\, \sigma_{V_\xi}^2}{V_x^4\left[r_a(2r_2 - r_1) \mp r_1 r_2 \frac{\lambda_S}{\lambda_L}\left(\frac{\overline{V}_\xi}{V_x}\right)^2\right]^4}$$

$$+ 4\left(\frac{\lambda_S}{\lambda_L}\right)^2 \frac{r_a^4\, r_1^2\, r_2^2(2r_2 - r_1)^2\, \overline{V}_\eta^2\, \sigma_{V_\eta}^2}{V_y^4\left[r_a(2r_2 - r_1) \mp r_1 r_2 \frac{\lambda_S}{\lambda_L}\left(\frac{\overline{V}_\eta}{V_y}\right)^2\right]^4} \qquad (170)$$

The expression for the variance is difficult to analyze unless computer techniques or valid approximations are employed. The latter method will be used to reduce the complexity of Eq. (170). If an electronic reference signal is used, then the distance r_2 is infinite. The electronic reference signal simulates a spherical source at infinity (i.e., plane wave of constant phase across the hologram). The second condition is to require a plane wave reconstruction source (i.e., $r_a = \infty$). Equation (170) can then be written as

$$V\left[r_b(V_\xi)ps + r_b(V_\eta)ps\right] \cong \left(\frac{\lambda_S}{\lambda_L} r_1\right)^2 \left[\left(\frac{L_\xi}{L_x}\right)^2 \frac{\sigma_{V_\xi}^2}{V_x^2} + \left(\frac{L_\eta}{L_y}\right)^2 \frac{\sigma_{V_\eta}^2}{V_y^2}\right] \qquad (171)$$

where

$$\frac{L_\xi}{L_x} = \frac{\overline{V}_\xi}{V_x}$$

and

$$\frac{L_\eta}{L_y} = \frac{\overline{V}_\eta}{V_y} \quad .$$

If the deviations in the simulated velocities are assumed never to exceed three standard deviations, then estimators of the variances can be defined by the following expressions:

$$\hat{\sigma}_{V_\xi}^2 = \frac{\Delta V_\xi^2}{9} \quad , \tag{172}$$

$$\hat{\sigma}_{V_\eta}^2 = \frac{\Delta V_\eta^2}{9} \quad . \tag{173}$$

Equation (171) reduces to the following expression

$$V\left[r_b(V_\xi)ps + r_b(V_\eta)ps\right] \cong \frac{1}{9}\left(\frac{\lambda_S}{\lambda_L} r_1\right)^2 \left[\left(\frac{L_\xi}{L_x}\right)^2 \frac{\Delta V_\xi^2}{\bar{V}_\xi^2} + \left(\frac{L_\eta}{L_y}\right)^2 \frac{\Delta V_\eta^2}{\bar{V}_\eta^2}\right]. \tag{174}$$

The standard deviation is

$$\sigma\left[r_b(V_\xi)ps + r_b(V_\eta)ps\right] \cong \frac{1}{3}\frac{\lambda_S}{\lambda_L} r_1 \sqrt{\left(\frac{L_\xi}{L_x}\right)^2 \frac{\Delta V_\xi^2}{\bar{V}_\xi^2} + \left(\frac{L_\eta}{L_y}\right)^2 \frac{\Delta V_\eta^2}{\bar{V}_\eta^2}} \quad . \tag{175}$$

THE EXPECTED VALUE OF THE IMAGE POINT POSITION

The expected or mean values of the image position are

$$E\left[r_b(V_\xi)ps\right] = \pm \frac{\lambda_S}{\lambda_L}\left(\frac{\bar{V}_\xi}{V_x}\right)^2 \left[\frac{r_a r_2 r_1}{r_a(2r_2 - r_1) \mp \frac{\lambda_S}{\lambda_L}\left(\frac{\bar{V}_\xi}{V_x}\right)^2 r_1 r_2}\right] \tag{176}$$

and

$$E\left[r_b(V_\eta)ps\right] = \pm \frac{\lambda_S}{\lambda_L}\left(\frac{\bar{V}_\eta}{V_y}\right)^2 \left[\frac{r_a r_2 r_1}{r_a(2r_2 - r_1) \mp \frac{\lambda_S}{\lambda_L}\left(\frac{\bar{V}_\eta}{V_y}\right)^2 r_1 r_2}\right] . \tag{177}$$

The stationary source expected values are given by similar expressions

$$E\left[r_b(V_\xi)ss\right] = \pm \frac{\lambda_S}{\lambda_L}\left(\frac{\overline{V}_\xi}{V_x}\right)^2 \left[\frac{r_a r_2 r_1}{r_a(r_2 - r_1) \mp r_1 r_2 \frac{\lambda_S}{\lambda_L}\left(\frac{\overline{V}_\xi}{V_x}\right)^2}\right] \tag{178}$$

and

$$E\left[r_b(V_\eta)ss\right] = \pm \frac{\lambda_S}{\lambda_L}\left(\frac{\overline{V}_\eta}{V_y}\right)^2 \left[\frac{r_a r_2 r_1}{r_a(r_2 - r_1) \mp r_1 r_2 \frac{\lambda_S}{\lambda_L}\left(\frac{\overline{V}_\eta}{V_y}\right)^2}\right] \tag{179}$$

If the stigmatic conditions are imposed, then the expected values of the image positions with respect to the velocity ratios $\frac{\overline{V}_\xi}{V_x}$ and $\frac{\overline{V}_\eta}{V_y}$ must be equal. This requires the velocity ratios to always be equal. It is the identical conditions that were imposed on the radial and lateral magnifications.

In acoustical scanned holography the reference source is usually generated electronically and with proper signal conditioning can simulate either a moving or stationary source. If we assume the reference source is a plane wave (i.e., $r_2 = \infty$) and impose the stigmatic conditions, then

$$E[r_b]ps = \pm \frac{\lambda_S}{\lambda_L}\beta^2 \left[\frac{r_1}{2 \mp \frac{r_1}{r_a}\frac{\lambda_S}{\lambda_L}\beta^2}\right] \tag{180}$$

where $\beta = \frac{\overline{V}_\xi}{V_x} = \frac{\overline{V}_\eta}{V_y}$. The stationary source expected value is

$$E[r_b]ss = \pm \frac{\lambda_S}{\lambda_L}\beta^2 \left[\frac{r_1}{1 \mp \frac{r_1}{r_a}\frac{\lambda_S}{\lambda_L}\beta^2}\right] . \tag{181}$$

It is interesting to note that if the reference and reconstruction sources are point sources at infinity (i.e., plane waves), then Eqs. (180) and (181) simplify to the following expressions:

$$E[r_b]ps = \pm \frac{\lambda_S}{\lambda_L} \frac{\beta^2 r_1}{2} \quad , \tag{182}$$

$$E[r_b]ss = \pm \frac{\lambda_S}{\lambda_L} \beta^2 r_1 \quad . \tag{183}$$

The ratio of the stationary source to the moving source image point is two. The expected value of the stationary source image position is twice as far from the hologram as the moving source image position. This means the image would appear closer or magnified in the moving source generated hologram. The image distance from the hologram is determined by the ratio of the sound to light wavelengths and the magnification of the hologram. If 1 MHz sound is used in the hologram construction and a helium neon laser in the reconstruction, then the image distance is approximately 2500 times the object distance assuming the magnification (i.e., $\beta = 1$). This means that a converging lens must be used with the hologram to have reasonable reconstruction distances. Figure 10 in the next section is a typical acoustic hologram reconstruction setup.

VIII. ACOUSTIC SCANNED HOLOGRAPHY SYSTEM

The experimental set-up used in the construction of the holograms is shown in Fig. 8. The apparatus is basically an x-y scanner with some unique signal conditioning features. Figure 9 is a picture of the scanner and associated electronics. The acoustic transmitter was either a plane-wave quartz crystal (5 cm in diameter) or a PZT-4 spherical ceramic (5 cm in diameter). The acoustic receiver was a PZT-5 ceramic (0.254 mm in diameter). The objects to be imaged were located outside of the periphery of the projected scanning aperture when stationary source illumination was employed and this allowed for complete separation of the two images (true, conjugate) and the undiffracted light. Objects can be placed inside the projected aperture, but the reference signal must be phase shifted or the source scanned to provided separation of the images.

The field of sound scattered or generated by the objects is scanned over a plane area by the receiving transducer. The area scanned (i.e., aperture) is usually about 10 cm x 10 cm with a line separation of 0.457 cm. The scanner is capable of varying both the aperture, line density and rate of scan. The receiver signals are amplified by a preamplifier located in close proximity to the receiving transducer. They are amplified again and then mixed with the electronic reference signal in a balanced mixer. This provides the necessary conditions for combining the received and reference signals in holography (see Appendix D). The output signal of the mixer is time-averaged, and the large voltage peaks are clipped before

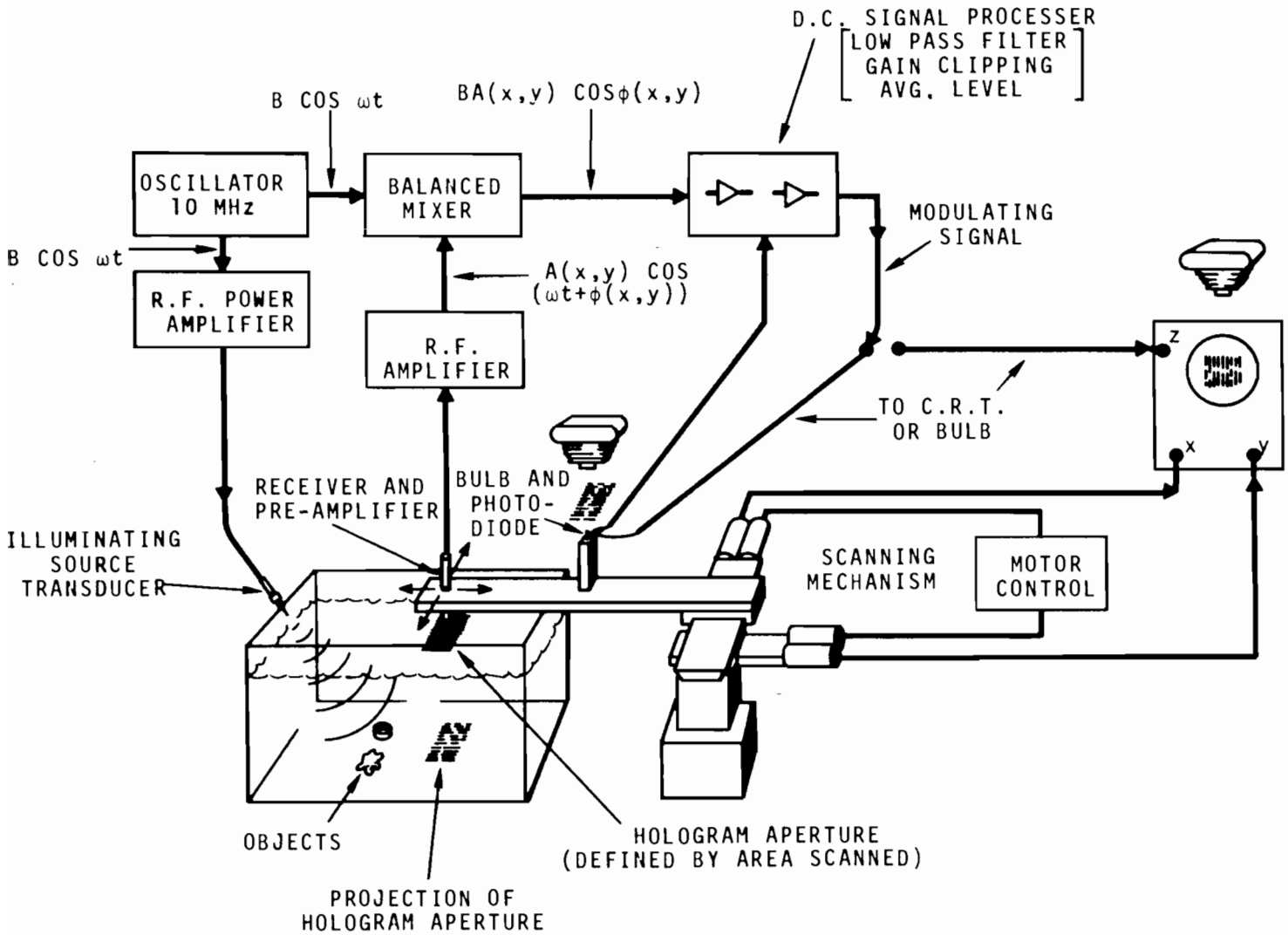

Figure 8. Ultrasonic hologram construction.

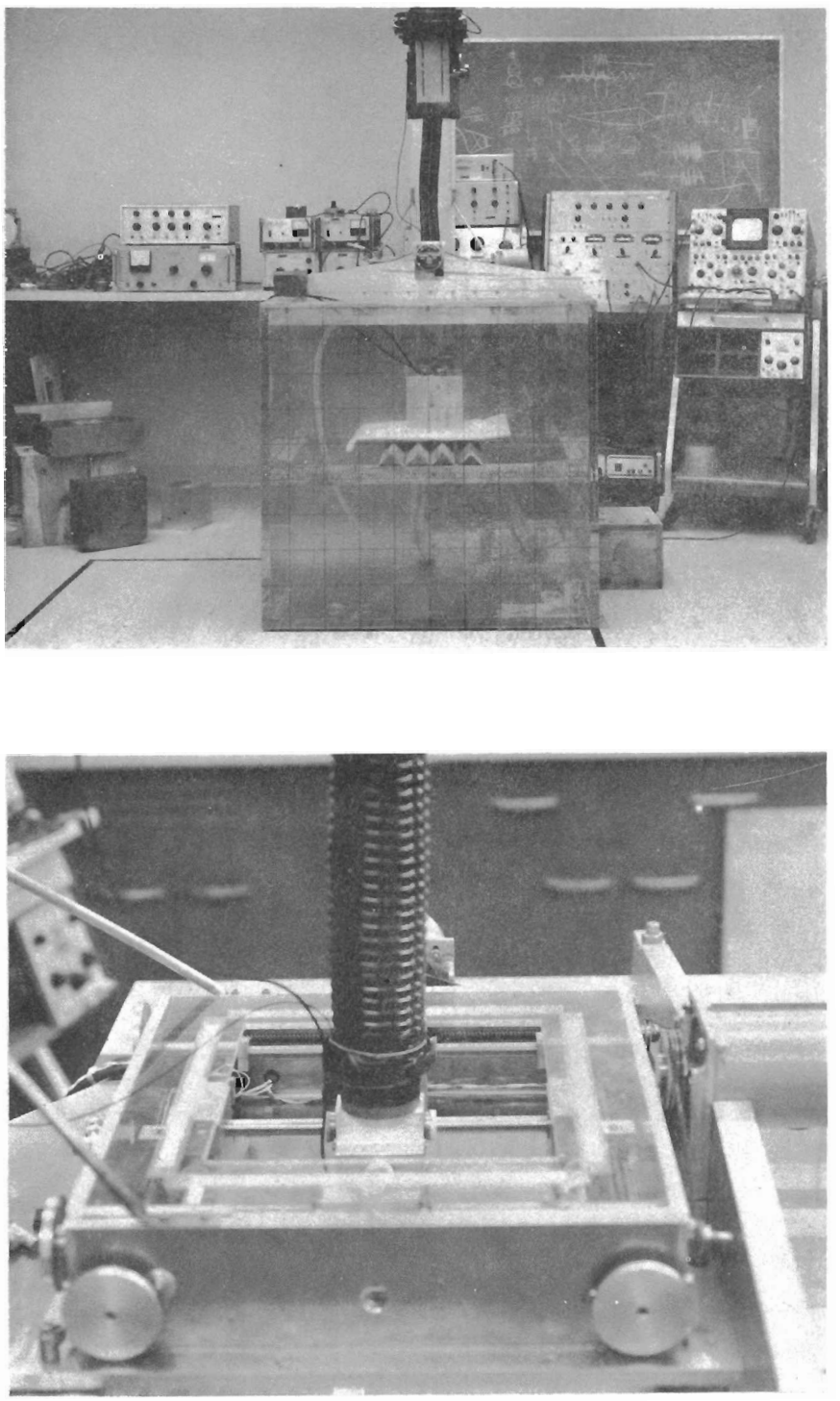

Figure 9. Holography scanner.

it is used to modulate the intensity of the glow modulator tube. The average level is adjusted to the center of the dynamic range of the light source and film sensitivity. The varying intensity of the modulator tube is coupled optically by a fiber optic light pipe to the top of the receiving transducer. A mirror located on the transducer reflects the light to a camera mounted above the scanning plane. The hologram is then constructed on 46L Polaroid transparency film. If the light source is mounted on the receiving transducer, then the scanning velocity and position errors are zero. Usually it is not possible in practical applications of acoustic holography to have the light source coupled directly to the scanning receiver. A cathode ray tube is used to construct the hologram and the receiver velocity components are simulated electronically to control the beam position. These signals contain errors that affect the hologram resolution, magnification, and image position.

HOLOGRAM RECONSTRUCTION GEOMETRY

Figure 10 shows the hologram reconstruction geometry. The helium-neon laser (6328 Å) is used after expanding the beam to completely illuminate the hologram. The lens was adjusted to bring the true image of the object into focus at 10 meters from the hologram. The lens had a focal length of 52 cm. The zero order (i.e., undiffracted light) and the conjugate image are then located between the true image and the hologram. The expected values of the hologram resolution, magnifications and image positions were verified experimentally using

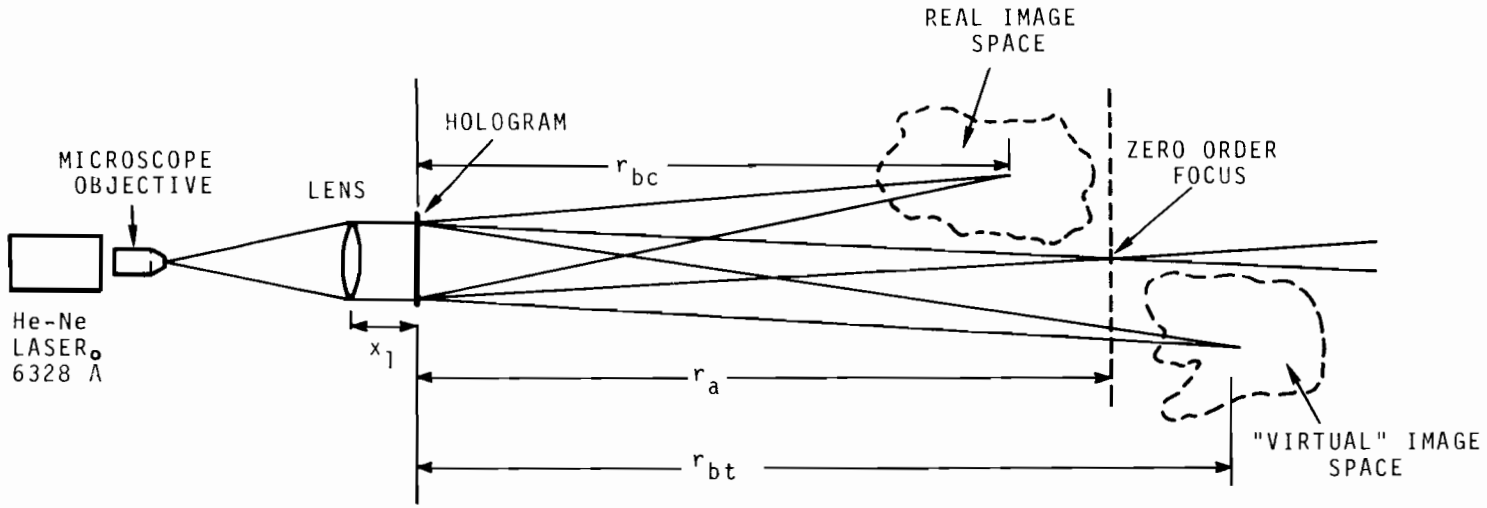

Figure 10. Hologram reconstruction geometry.

this reconstruction geometry. The expected value image positions of the objects were in excellent agreement with the theoretical calculations. Positioning of the lens determined the depth of focus in the hologram. Objects at various depths in the tank came into focus at different lens positions. The expected value of the lateral and radial magnifications were calculated from the theory and proven to agree with the experimental results.

IX. EXPERIMENTAL RESULTS

In this section we describe a number of experiments to verify some of the theoretical results developed in the preceeding sections. The expected value of the hologram resolution, radial, lateral magnifications, and image position are proven to agree conclusively with the theory. The experiments include stationary source illumination (i.e., receiver scanning alone) and simultaneous source receiver scanning.

HOLOGRAM RESOLUTION EXPERIMENTS

The initial experiments were designed to verify the expected value of the hologram resolution employing both stationary and moving source illumination. Two 0.25 mm diameter PZT-5 ceramic transducers were mounted side by side in the water tank outside of the projected aperture. The lateral separation, object to hologram distance, aperture and the acoustic frequency were set according to Eq. (69). Numerous holograms were constructed using the same technique and varying the parameters that effect the resolution. Figure 11 shows a hologram and the reconstruction of the true image. In this example the lateral separation was 5.1 mm, line density 22 lines/cm, object to hologram distance 31 cm, frequency 3.6 MHz and the scanning aperture 2.54 cm x 2.54 cm. The two images in the reconstruction are almost touching and the two points can be identified. Now if we decrease the lateral separation, the two points would be unresolvable in the reconstruction and we have exceeded the resolution of the

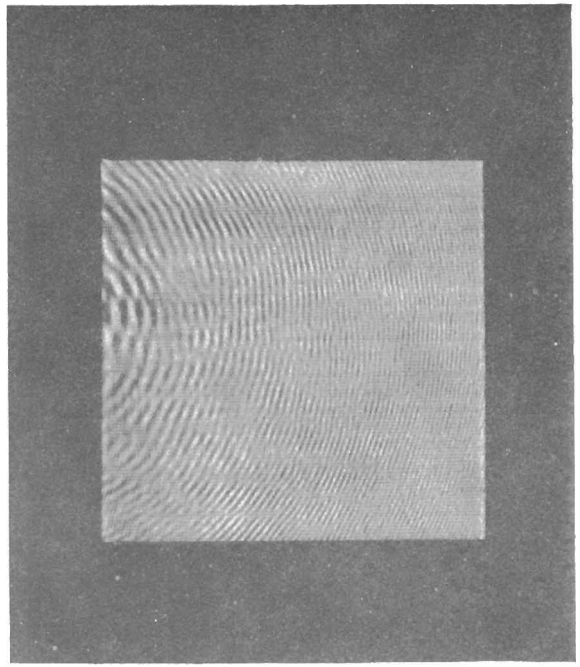

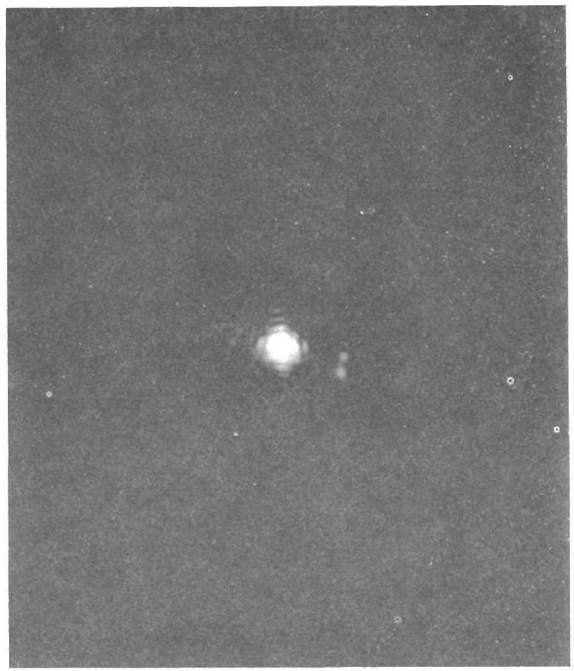

Acoustic Hologram		True Image at 10 meters	
Illumination:	Stationary Source	Objects:	9.5 mm diameter styrofoam disks
Frequency:	3.6 Mhz	Object Lateral Separation:	5.1 mm
Film Magnification:	2	Resolution:	5.1 mm
Line Density:	22 lines/cm	Aperture:	2.54 cm x 2.54 cm

Figure 11. Hologram and reconstruction of two circular objects.

hologram. The optical system used in the reconstruction is shown in Fig. 10. The reconstruction distance x_1 = 5.9 cm, d_0 = 560 cm, r_{bt} = 1000 cm and r_{bc} = 390 cm.

Increasing the frequency or the aperture increased the resolution as shown in Fig. 12. The two images are now completely separated. The resolution measurements were obtained and checked using this technique. Figure 13 is a family of curves showing the stationary source hologram resolution as a function of object to hologram distance and aperture size. Figure 14 shows the hologram and the reconstruction of the true image. The source and receiver were scanned together and the image separation distance has increased approximately twice the stationary source image separation distance (see Fig. 11). This experimental result proves conclusively that simultaneous source receiver scanning doubles the resolution capability. Figure 15 is a family of curves showing the hologram moving source resolution as a function of object to hologram distance and aperture dimension. The source and receiver were scanned simultaneously together. This increased the hologram resolution by a factor of two (i.e., decreased the resolvable distance). Intuitively, the reason for this increase in resolution can be explained in the following way. In a stationary source hologram the receiver is cutting across the acoustic spherical wavefronts reflected from a point object. The hologram becomes the familiar zone plate with a line density proportional to the rate of change of the object to receiver distance. If the source moves, the illumination angle changes at the same rate as the receiver and this

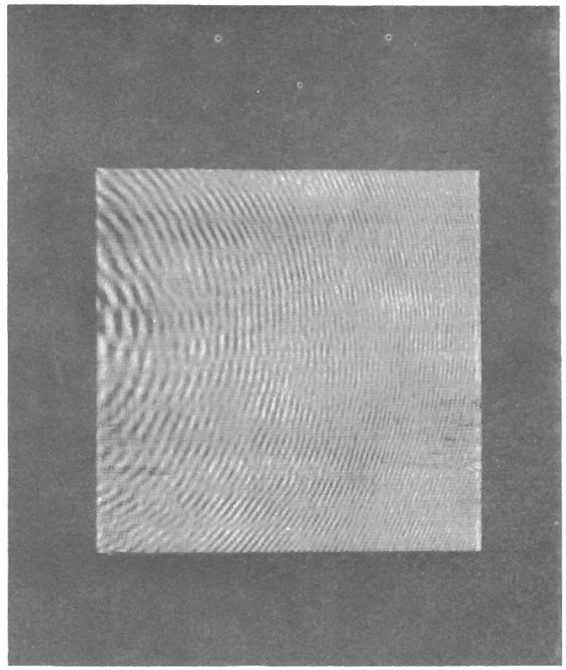

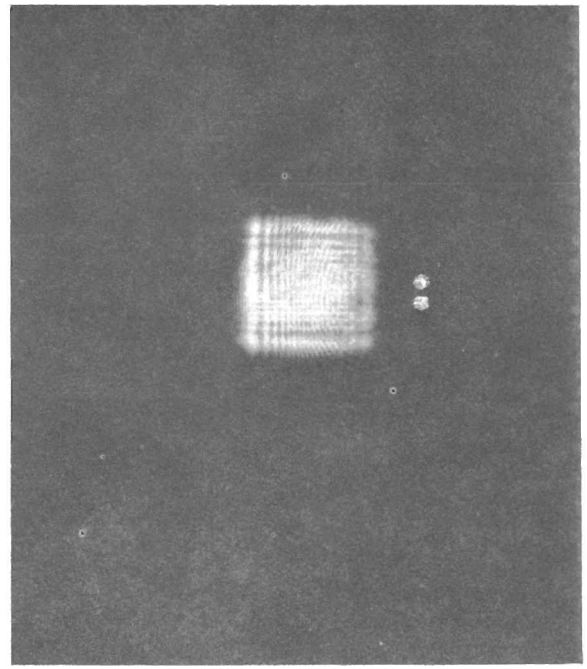

Acoustic Hologram		True Image at 10 meters	
Illumination:	Stationary Source	Objects:	9.5 mm diameter styrofoam disks
Frequency:	3.6 Mhz	Object Lateral Separation:	5.1 mm
Film Magnification:	2	Resolution:	1.27 mm
Line Density:	22 lines/cm	Aperture:	10 cm x 10 cm
		Lateral Magnification:	0.196

Figure 12. Hologram and reconstruction of two circular objects.

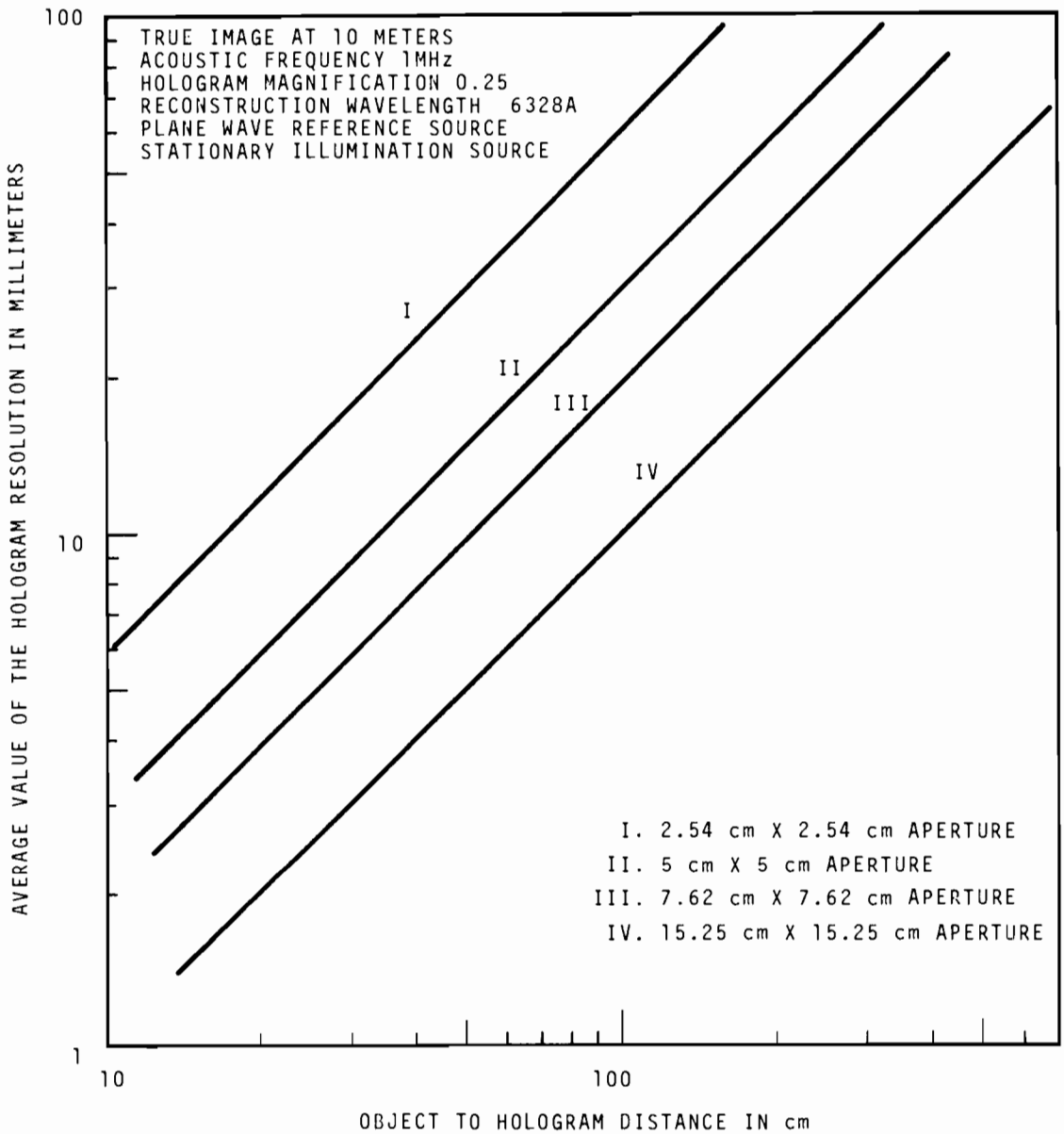

Figure 13. Stationary source hologram resolution.

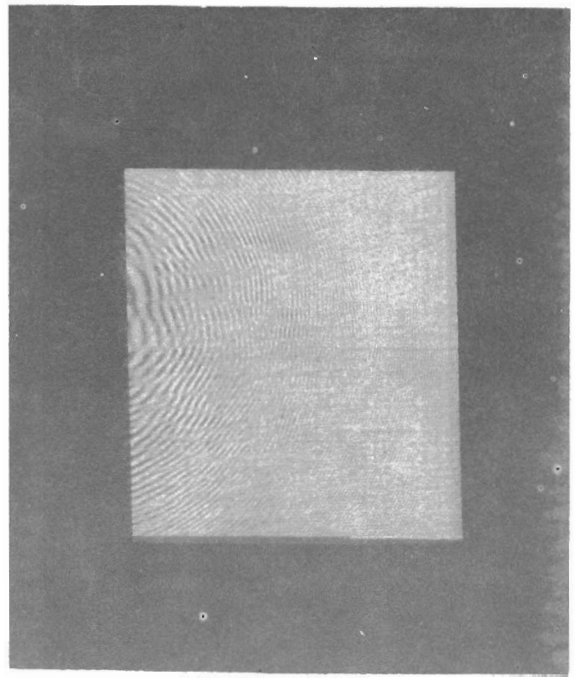

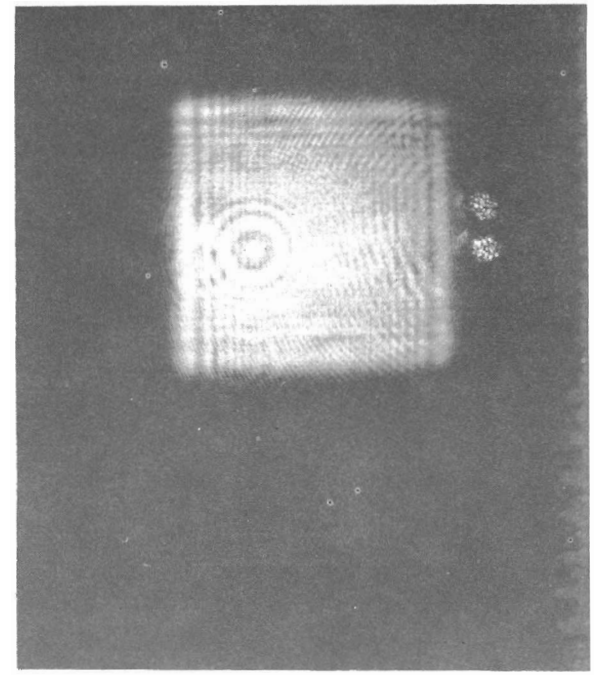

Acoustic Hologram

Illumination:	Moving Point Source
Frequency:	3.6 Mhz
Film Magnification:	2
Line Density:	22 lines/cm

True Image at 10 meters

Objects:	9.5 mm diameter styrofoam disks
Object Lateral Separation:	5.1 mm
Resolution:	0.635 mm
Aperture:	10 cm x 10 cm
Lateral Magnification:	0.392

Figure 14. Hologram and reconstruction of two circular objects.

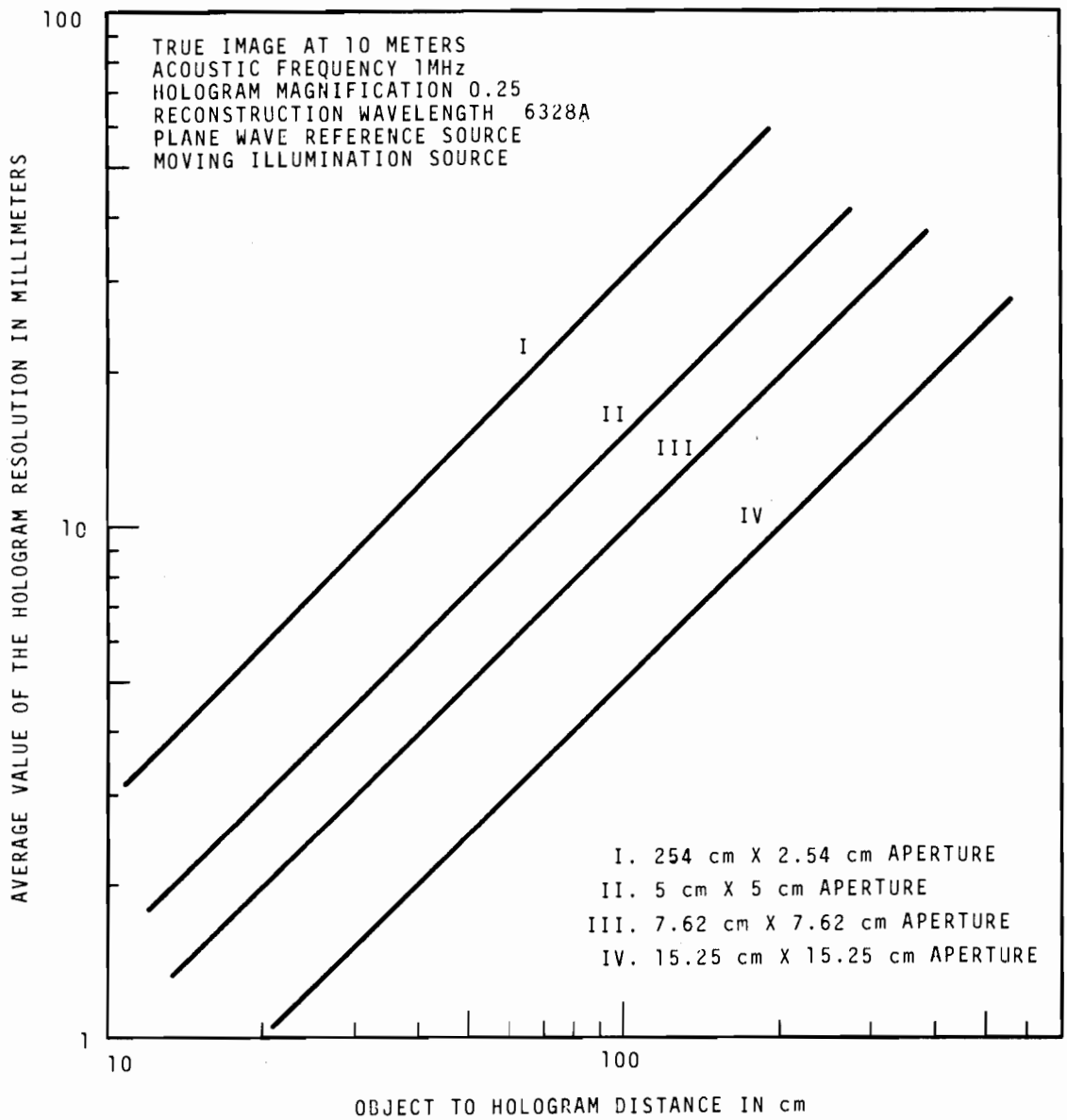

Figure 15. Simultaneous source receiver scanned hologram resolution.

increases the line density to approximately twice its former value. Thus, for a hologram of a general object the spatial bandwidth has approximately doubled when simultaneous source-receiver scanning is used.

RADIAL MAGNIFICATION EXPERIMENTS

The experiments were designed to verify the expected value of the stationary and moving source radial magnification. Two point objects were separated at various distances in the radial direction (i.e., depth). Holograms were constructed at different frequencies and objects distances. Figure 16 shows a hologram and the reconstructions of the two point objects. The hologram was constructed at 3.6 MHz, the radial separation 5 cm, the line density 22 lines/cm, the scanning aperture 10 cm x 10 cm, the object to hologram distances 30.5 cm and 35.5 cm. The upper image (i.e., circular dot) is in focus 1000 cm from the hologram. In Fig. 17 the lower image is in focus 900 cm from the hologram. The difference in the object to hologram distances was calculated and agreed with the theoretical value of the radial magnification. The true images were viewed at approximately 10 meters using the optical system as shown in Fig. 10. The reconstruction distances for the upper image were x_1 = 5.8 cm, d_0 = 560 cm, r_{bt} = 1000 cm and r_{bc} = 390 cm. The reconstruction distances for the lower image were x_1 = 5.8 cm, d_0 = 560 cm, r_{bt} = 900 cm, and r_{bc} = 4.6 cm. Figure 18 shows a family of curves of the stationary source hologram radial magnification as a function of frequency and object to hologram distance. Radial magnification measurements were obtained using

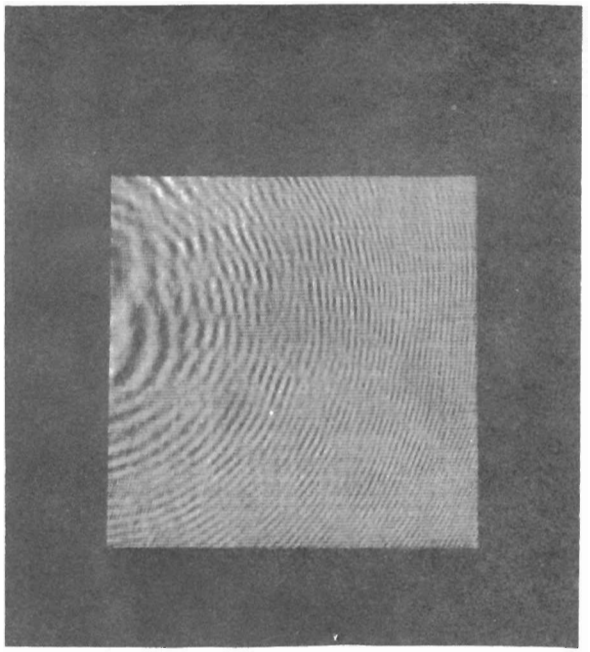

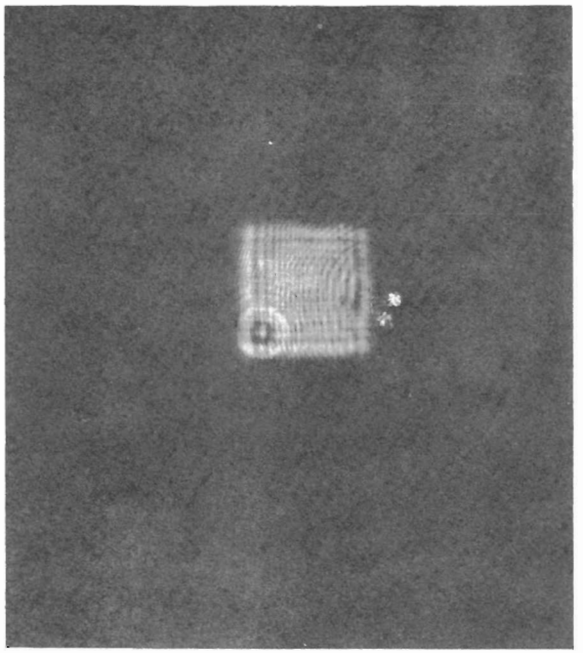

Acoustic Hologram

Illumination:	Stationary Source
Frequency:	3.6 Mhz
Film Magnification:	2
Line Density:	22 lines/cm

True Image at 10 meters

Objects:	9.5 mm diameter styrofoam disks
Objects Radial Separation:	5 cm
Aperture:	10 cm x 10 cm
Radial Magnification:	20

Figure 16. Hologram and the reconstruction of two circular objects separated in the radial direction.

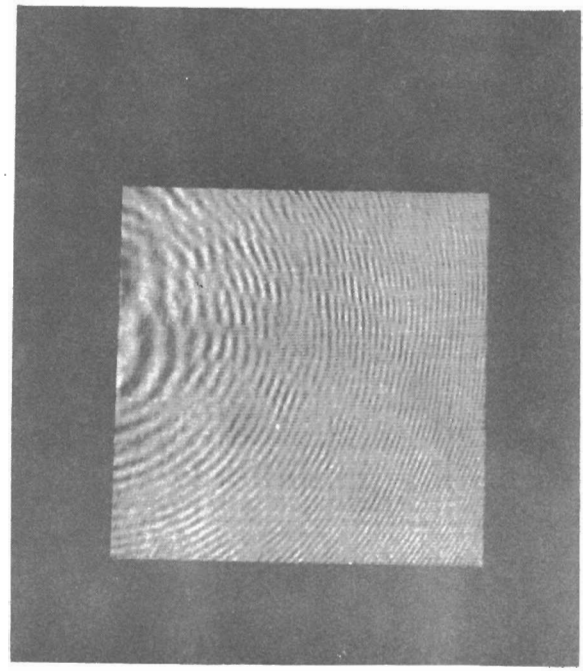

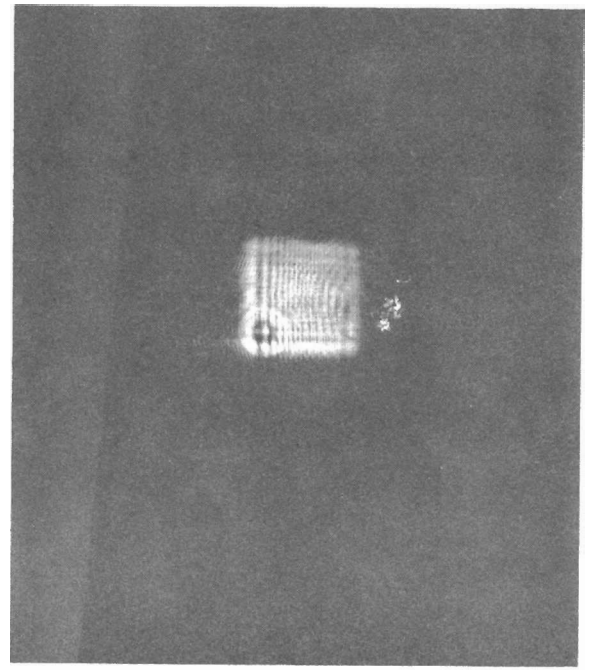

Acoustic Hologram		True Image at 9 meters	
Illumination:	Stationary Source	Objects:	9.5 mm diameter styrofoam disks
Frequency:	3.6 Mhz	Objects Radial Separation:	5 cm
Film Magnification:	2	Aperture:	10 cm x 10 cm
Line Density:	22 lines/cm	Radial Magnification:	20

Figure 17. Hologram and the reconstruction of two circular objects separated in the radial direction.

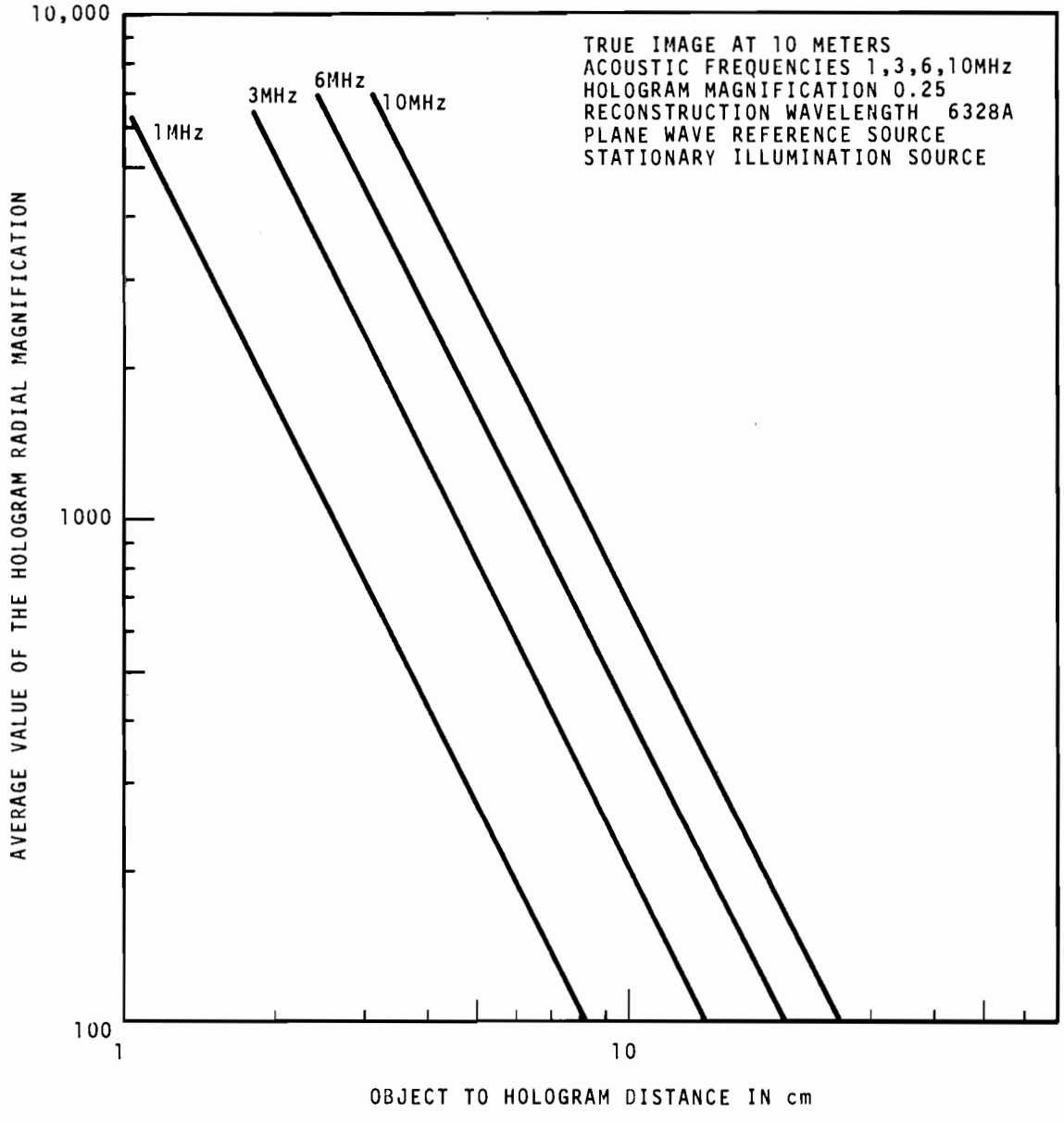

Figure 18. Hologram stationary source radial magnification.

simultaneous source receiver scanning. The radial magnification was decreased by a factor of two, which agreed with the theoretical prediction. Figure 18a shows a family of curves of the moving source radial hologram magnification as a function of frequency and object to hologram distance.

HOLOGRAM LATERAL MAGNIFICATION EXPERIMENTS

The experiments were designed to verify the expected value of the lateral hologram magnification using stationary and moving source illumination. Two circular objects were separated at various distances in the lateral direction. Holograms were constructed at different frequencies and object distances. Figure 12 shows a hologram and the reconstruction of the true image. The hologram was constructed at 3.6 MHz, the lateral separation 5.1 mm, the line density 22 lines/cm, the scanning aperture 10 cm x 10 cm, and the object to hologram distance 31 cm. The reconstruction distances were x_1 = 5.9 cm, d_0 = 560 cm, r_{bt} = 1000 cm and r_{bc} = 390 cm. The expected value of the lateral magnification was calculated by taking the ratio of the lateral separation distance between the two images in the reconstruction and the lateral separation distance between the objects. The true image was viewed at 10 meters from the hologram using the optical system shown in Fig. 10. The results were in excellent agreement with the theoretical calculations. Figure 19 shows a family of curves of the stationary source hologram magnification as a function of frequency and object to hologram distance. Lateral magnification measurements were obtained using simultaneous source receiver scanning and the

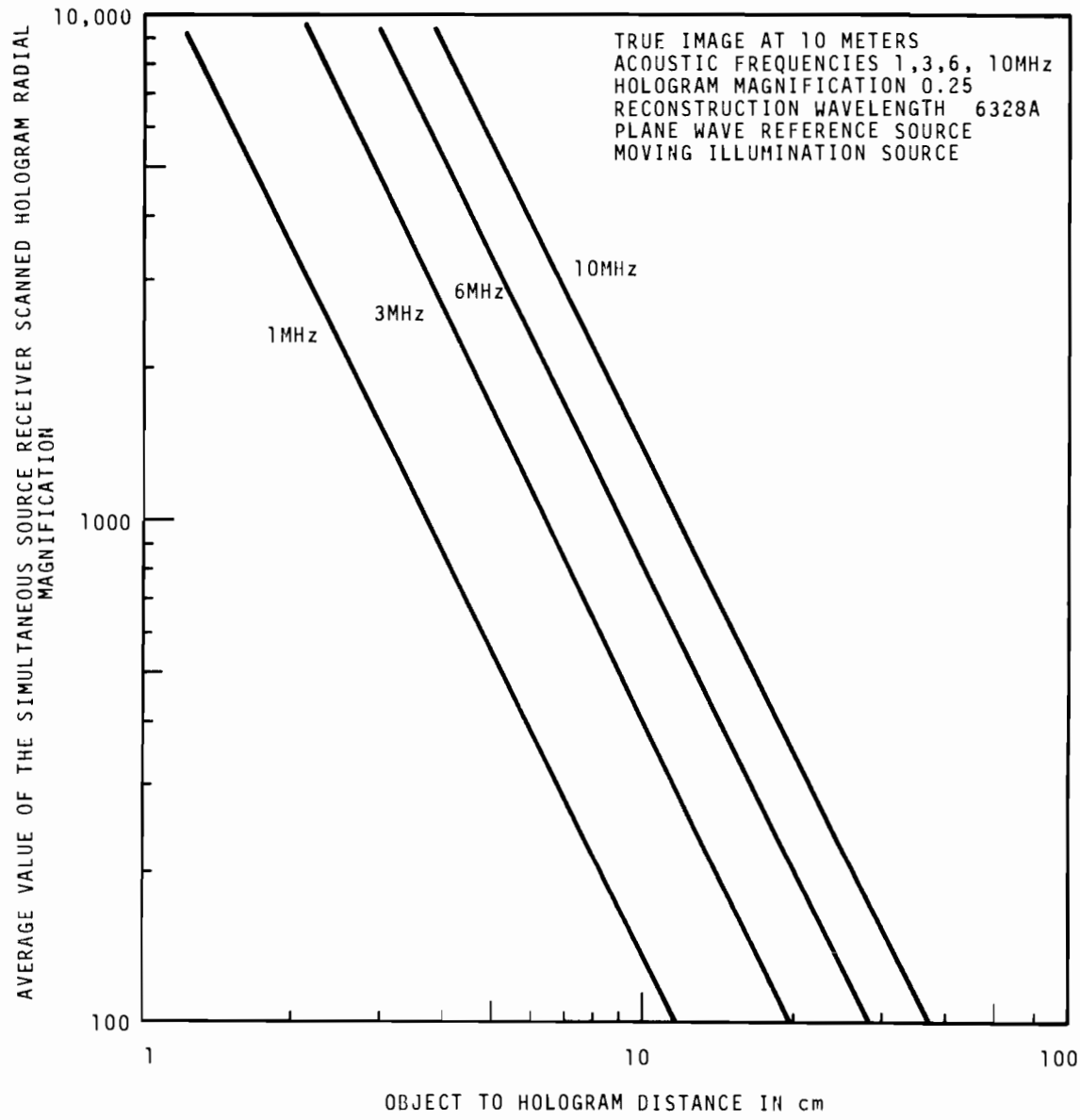

Figure 18a. Hologram moving source radial magnification.

results verified the theoretical calculations. Figure 20 shows the stationary source hologram and the reconstruction of the true image at 10 meters from the hologram. The object was to show by comparison with the stationary source hologram that scanning the source and receiver decreases the image distance (i.e., $r_b \approx \bar{r}_{b/2}$). The object was a styrofoam figure "F". The hologram was constructed at 3.6 MHz, the line density 22 lines/cm, the scan aperture 10 cm x 10 cm, and the object to hologram distance 28 cm. The length of the figure was 4.9 cm and the width 3.18 cm. The reconstruction distances were x_1 = 5.9 cm, d_0 = 560 cm, r_{bt} = 1000 cm and r_{bc} = 390 cm. Figure 21 shows the moving source hologram and the reconstruction of the true image at 10 meters from the hologram. The image of the figure "F" is approximately twice the size of the stationary source hologram image. This result shows that the lateral magnification is the same and the image size would be identical to the stationary source image (figure 20) if viewed at approximately 5 meters. The reconstruction distances were x_1 = 5.9 cm, d_0 = 560 cm, r_{bt} = 1000 cm and r_{bc} = 390 cm. Figure 22 shows a family of curves of the moving source lateral hologram magnification as a function of frequency and object to hologram distance. The true images were viewed at 10 meters from the hologram.

HOLOGRAM IMAGE POSITION EXPERIMENTS

The experiments were designed to verify the expected value of the image position using stationary and moving source illumination. Objects were placed at various depths in the tanks. Holograms were constructed at different frequencies and object distances. The

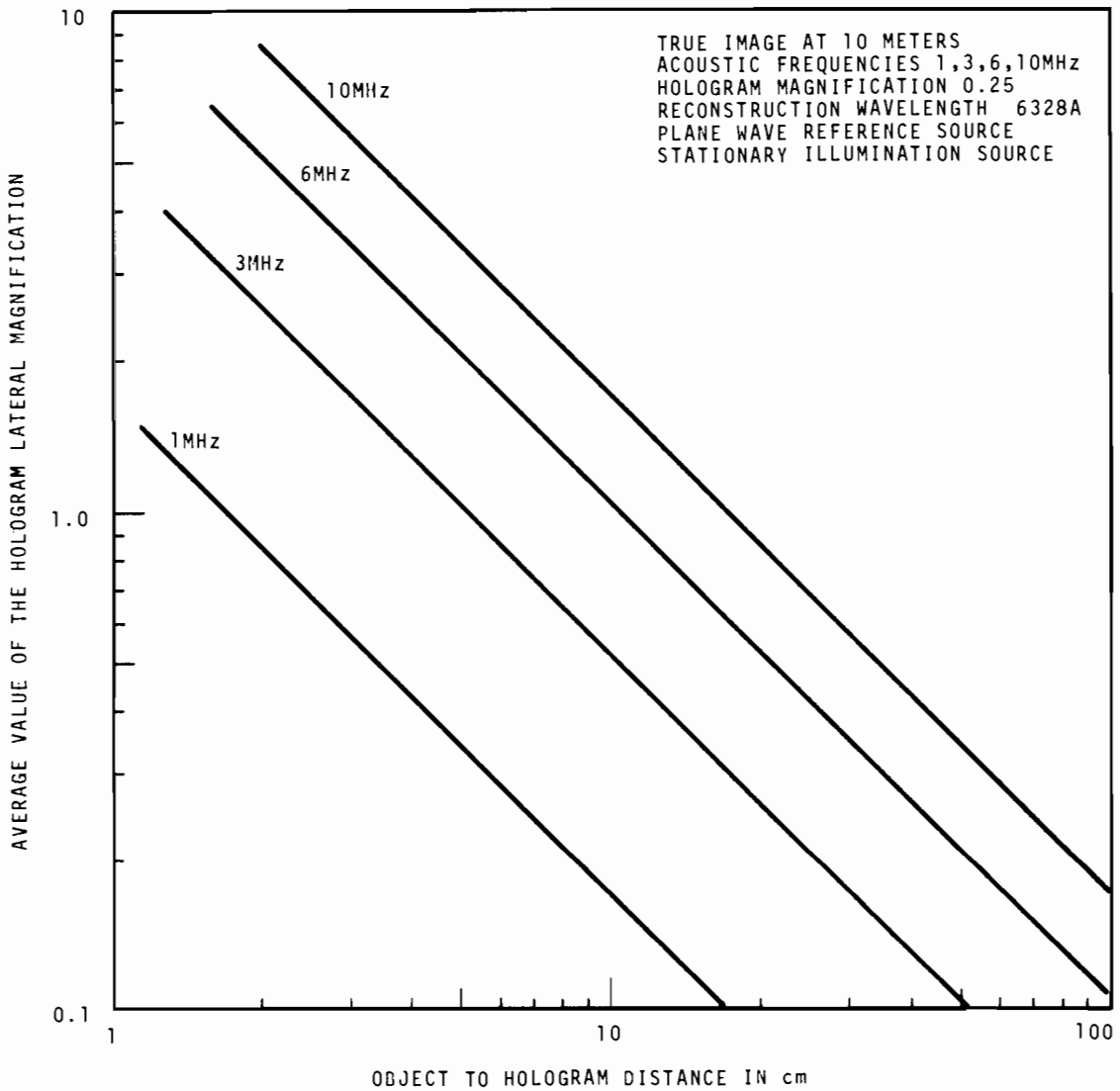

Figure 19. Hologram stationary source lateral magnification.

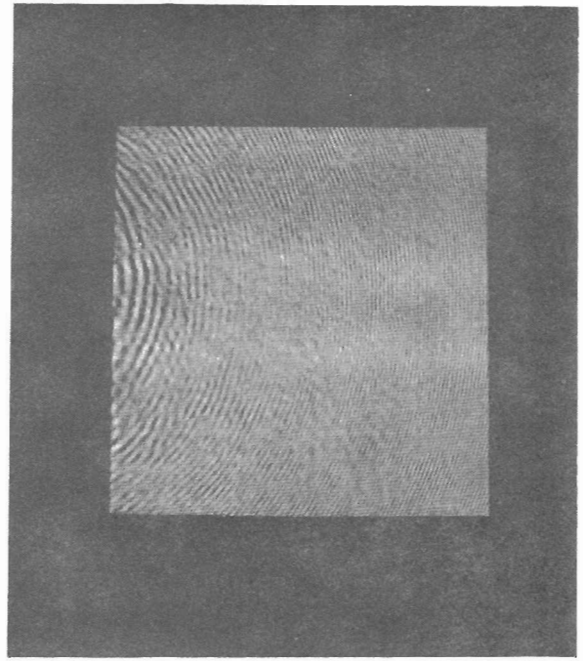

Acoustic Hologram

Illumination:	Stationary Source
Frequency:	3.6 Mhz
Film Magnification:	2
Line Density:	22 lines/cm

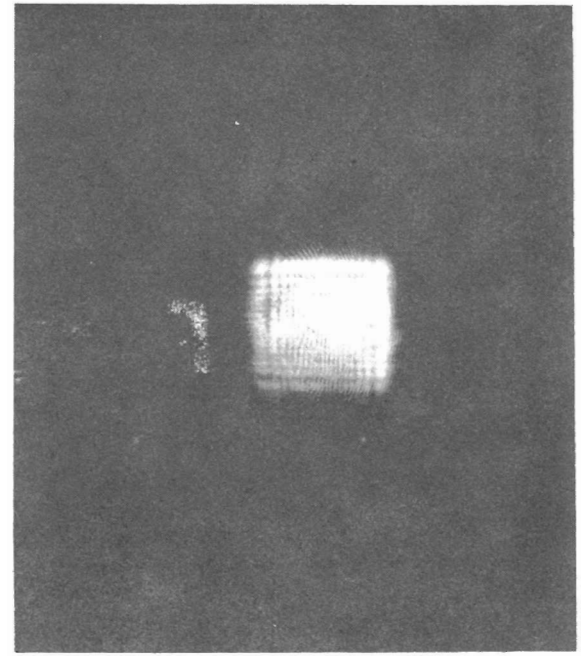

True Image at 10 meters

Object:	Styrofoam "F"
Resolution:	1.16 mm
Aperture:	10 cm x 10 cm
Lateral Magnification:	0.217

Figure 20. Hologram and reconstruction of the figure "F".

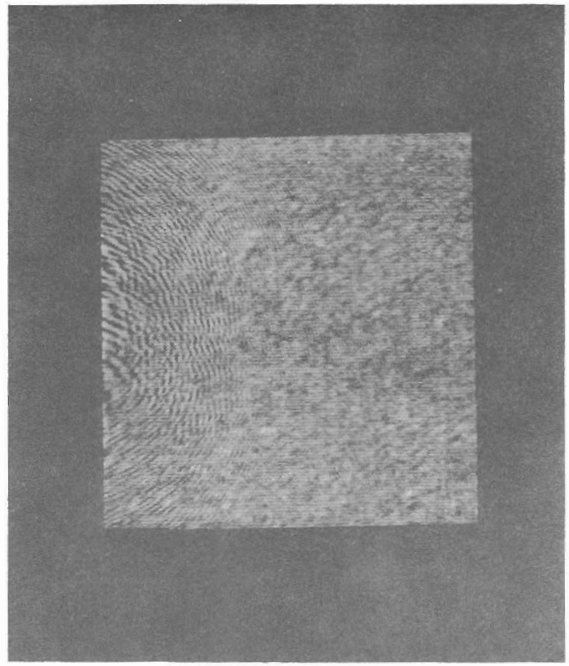

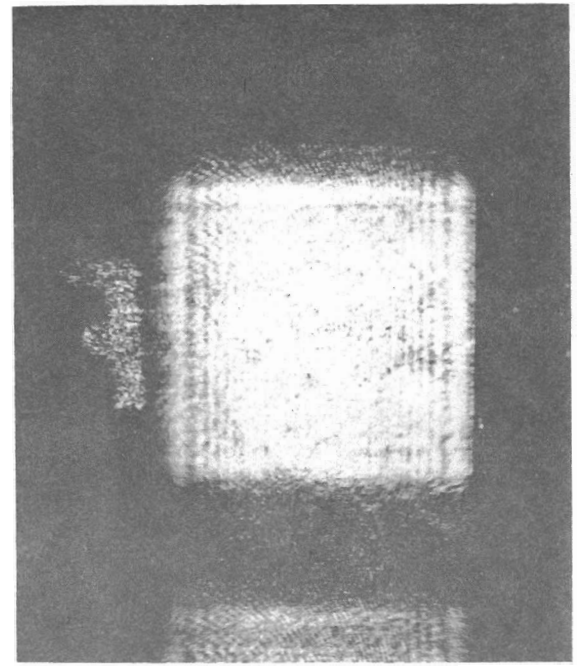

Acoustic Hologram		True Image at 10 meters	
Illumination:	Moving Point Source	Object:	Styrofoam "F"
Frequency:	3.6 Mhz	Resolution:	0.58 mm
Film Magnification:	2	Aperture:	10 cm x 10 cm
Line Density:	22 lines/cm	Lateral Magnification:	0.434

Figure 21. Hologram and reconstruction of the figure "F".

expected values of the image positions were measured using the optical system shown in Fig. 10. Figure 20 shows a stationary source hologram and the reconstruction of the true image. The expected value of the true image position (i.e., r_{bt}) was 1000 cm. The expected value of the conjugate image position was 390 cm. Numerous image positions were measured and the results agreed with the theoretical calculations. Figure 21 shows a moving source hologram and the reconstruction of the true image. The expected value of the true image position was 1000 cm. The expected value of the conjugate image position was cm. Figure 23 shows a moving plane-wave source hologram and the reconstruction of the true and conjugate images. The styrofoam figure "F" was placed directly in the projected scanning aperture. The plane-wave transducer was inclined at 10 degrees with the horizontal and the image was shifted approximately 6 cm from the undiffracted light. The hologram was constructed at 4.75 MHz, the line density 22 lines/cm, the scanning aperture 15 cm x 15 cm, and the object to hologram distance 33 cm. The expected values of the true and conjugate images were 1000 cm and 365 cm, respectively, with the zero order focussed at 540 cm. The theoretical calculation of image positions were in good agreement with the experimental results.

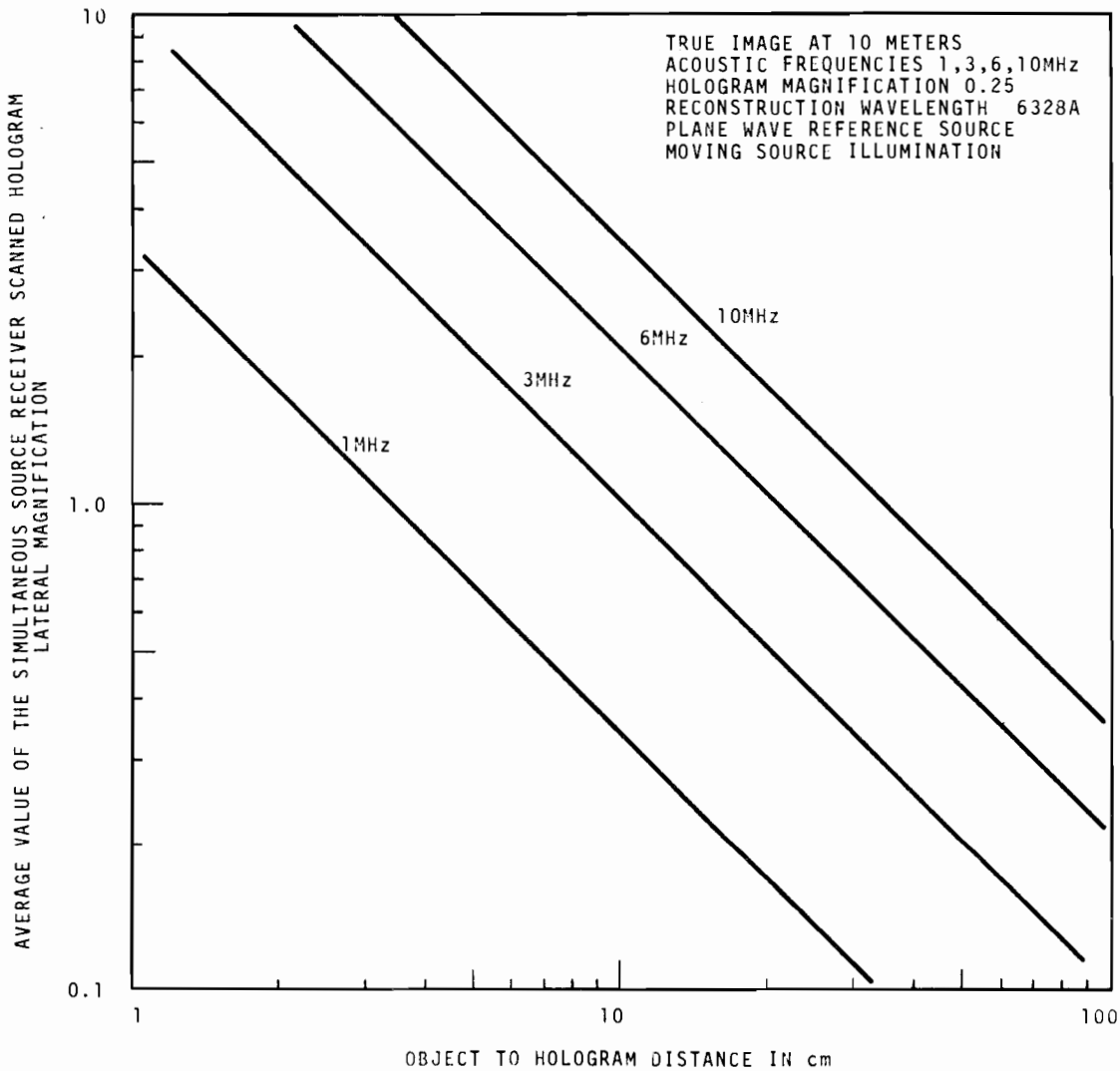

Figure 22. Hologram moving source lateral magnification.

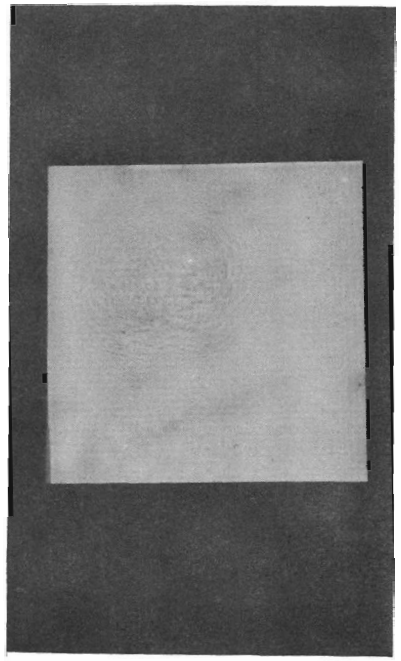

Acoustic Hologram
Illumination: Moving Plane-Wave Source
Frequency: 4.75 Mhz
Film Magnification: 2
Line Density: 22 lines/cm

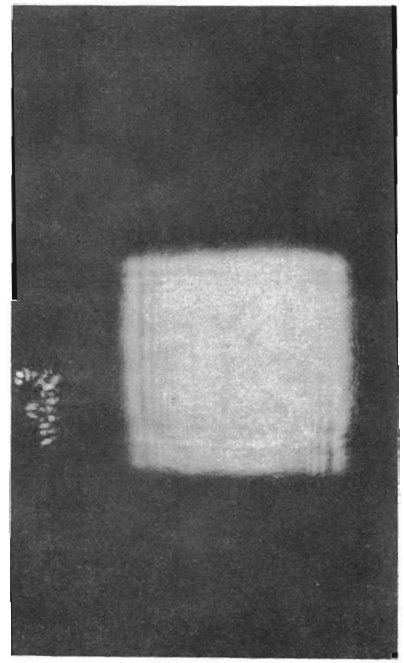

True Image at 10 meters
Object: Styrofoam "F"
Resolution: 0.7 mm
Aperture: 15 cm x 14 cm
Lateral Magnification: 0.24

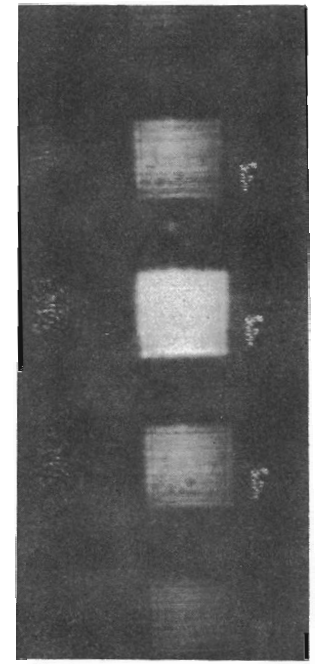

Conjugate Image at 3.65 Meters
Object: Styrofoam "F"
Resolution: 0.7 mm
Aperture: 15 cm x 15 cm
Lateral Magnification: 0.0875

Figure 23. Hologram and the reconstructions.

X. SUMMARY AND CONCLUSIONS

In this thesis we have presented a generalized analysis of scanning errors in acoustic holography. The analysis includes simultaneous source receiver scanning and receiver scanning alone. These errors adversely affect the hologram resolution, magnifications (radial, lateral) and the image position. The simulated velocity and position errors are assumed to be statistically independent, identically distributed random variables; i.e., random variables with the same distribution function.

The law of propagation of errors for the general case (i.e., for several random variables) is used in the analysis. Its validity is based on the assumption that the errors are reasonably small with respect to the measured values of the variables. In practice, if the standard deviation is of the order of 10% of the measured value of the variable, the law can be reliably used. The approximate variance, standard deviation and expected values are derived for the hologram resolution, magnifications (i.e., radial, lateral) and image positions using simultaneous source receiver scanning and receiver scanning alone.

The standard deviation of the hologram resolution varied inversely as the square of the aperture dimension and this implied that increasing the scanning aperture greatly reduced the resolution errors. Demagnification of the hologram also increased the resolution errors and the errors increased directly with the wavelength of sound and the position error. Scanning both the source and receiver decreased the

resolution errors by a factor by two compared with the stationary source resolution. The expected value of the hologram resolution was increased by a factor of two compared with the stationary source resolution. Thus, simultaneous source scanning increased the resolution and decreased the standard deviation.

The standard deviation of the hologram radial and lateral magnifications varied directly as the deviation in the simulated receiver velocity for simultaneous source receiver scanning and receiver scanning alone. The standard deviation in the radial magnification was decreased by simultaneous source receiver scanning and the ratio of the standard deviations of the radial magnifications [i.e., $^{\sigma}M_R(ss)/^{\sigma}M_R(ps)$] was approximately two.

The standard deviation of the hologram image position varied directly as the sound to light wave length ratio and object to hologram distance. Scanning both the source and receiver decreased the standard deviation by a factor of two compared with the stationary source standard deviation. Thus, simultaneous source receiver scanning decreased the standard deviation in hologram resolution, radial magnification, and image position, but remained the same in the lateral magnification. The expected value of the simultaneous source receiver hologram image position is decreased by a factor of two compared with the stationary source image position if a plane-wave source is used in the reconstruction (i.e., $r_b \approx \bar{r}_{b/L}$). Thus, scanning both the source and receiver together makes the object appear closer to the hologram plane.

Experimental results for the expected values of hologram resolution, magnifications (i.e., radial and lateral) and image position are shown. Various graphs have been plotted and the results are in good agreement with the theory.

BIBLIOGRAPHY

1. Gabor, Dennis. A new microscopy principle. Nature 161:777-778. 1948.

2. Gabor, Dennis. Microscopy by reconstructed wavefronts. Proceedings of the Royal Society. A197:454-456. 1949.

3. Gabor, Dennis. Microscopy by reconstructed wavefronts. Proceedings of the Physical Society. B64:499-500. 1951.

4. Leith, Emmett and Upatnicks, Juris. Reconstructed wavefronts and communication theory. Journal of the Optical Society of America. 52:1123-1130. 1962.

5. Leith, Emmett and Upatnicks, Juris. Wavefront reconstruction with continuous tone objects. Journal of the Optical Society of America. 53:1377-1381. 1963.

6. Leith, Emmett and Upatnicks, Juris. Wavefront reconstruction with diffused illumination and three dimensional objects. Journal of the Optical Society of America. 54:1295-1301. 1964.

7. Metherell, A. F., El-Sum, H. M., and Larmore, Lewis. Acoustical Holography. New York, Plenum Press, 1969, 294 p.

8. Hildebrand, Percy, Unpublished research on acoustical holography. Richland, Washington, Applied Physics Department of Battelle-Northwest, 1967.

9. Metherell, A. F., El-Sum, H. M., Dreher, J. and Larmore, Lewis. Journal of the Acoustical Society of America. 42:733. 1967.

10. Goodman, Joseph W.. Introduction to fourier optics. New York, McGraw-Hill, 1968. 287 p.

11. Haines, Kenneth. The analysis and application of hologram interferometry. Doctoral dissertation. Ann Arbor, University of Michigan, 1966. 99 numb. leaves.

12. Hildebrand, Percy. Unpublished research on source receiver scanning in acoustical holography, Richland, Washington, Applied Physics Department of Battelle-Northwest, 1969.

13. Champagne, E. B.. Journal of the Optical Society of America. 57:51-53. 1967.

14. Hildebrand, Percy and Haines, Kenneth. Holography by scanning. Journal of the Optical Society of America. 59:1-6. 1969.

APPENDICES

APPENDIX A

THE LAW OF PROPAGATION OF ERRORS

The exact calculation of the variance of a nonlinear function containing several variables that are subject to error is generally a problem of considerable mathematical complexity. Generally, approximations are used and it is not necessary to solve these difficult problems exactly. There exists a process called linearization that allows the replacement of any nonlinear function with a linear one, for the purpose of obtaining approximate estimates of the variances. The approximation is usually quite adequate for most applications. Linearization is based on the Taylor's series expansion of the nonlinear function with retention of only the linear portion of the expansion.

Let us consider first a function of a single random variable:

$$M = f(X) \quad .$$

For example, X might represent the simulated scanning velocity of the receiver and M its magnification. We are interested in the random error of M as a result of random errors in X.

To an error ε in X, corresponds an error δ in M, given by

$$\delta = f(X + \varepsilon) - f(X) \quad . \tag{A-1}$$

If we assume ε to be small with respect to X, it can be treated as a differential increment. Then the following approximation is assumed valid

$$\frac{f(X + \varepsilon) - f(X)}{\varepsilon} \approx \frac{df(X)}{dX} \tag{A-2}$$

and

$$\delta = \frac{df(X)}{dX}\,\varepsilon = \frac{dM}{dX}\,\varepsilon \tag{A-3}$$

where the derivative of M with respect to X is evaluated at the measured or average value of X. The variance is given by the following expression

$$V(\delta) = \left(\frac{dM}{dX}\right)^2 V(\varepsilon) \tag{A-4}$$

where $\frac{dM}{dX}$ is a constant.

For example, consider the lateral hologram magnification

$$M_L(x)ss = \mp \frac{\lambda_L}{\lambda_S}\frac{V_x}{V_\xi}\frac{r_b}{r_1} \quad . \tag{A-5}$$

The derivative with respect to the velocity V_ξ is

$$M_L'(x)ss = \mp \frac{\lambda_L}{\lambda_S}\frac{V_x}{V_\xi^2}\frac{r_b}{r_1} \tag{A-6}$$

and the variance

$$V(\delta) = \left(\frac{\lambda_L}{\lambda_S}\frac{V_x}{\overline{V}_\xi^2}\frac{r_b}{r_1}\right)^2 V(\varepsilon_\xi) \tag{A-7}$$

where ε is the random error in the velocity simulation, and δ the random error, induced by ε, in the magnification. If $\varepsilon_V \sim N(0,\sigma_\varepsilon^2)$, then the standard deviation is

$$\sigma\delta = \frac{\lambda_L}{\lambda_S}\frac{V_x}{V_\xi^2}\frac{r_b}{r_1}\,\sigma_\varepsilon \quad . \tag{A-8}$$

Expressing the error as a coefficient of variation, we have

$$\% \text{ C } V_{M_L} = \frac{\sigma_\varepsilon}{\overline{V}_\xi} \times 100 \quad . \tag{A-9}$$

Equation (A-4) expresses the law of propagation of errors for the case of a single independent variable. Its proof is based on the assumption that the error ε is small with respect to the measured value of x (i.e., $\sigma_\varepsilon < 0.1$ of x).

The law of propagation of errors for the case of several random variables is just an extension of Eq. (A-4). Assume

$$u = f(x,y,z, \ldots) \tag{A-10}$$

where x,y,z . . . represent random variables. Let ε_1, ε_2, ε_3, . . . represent statistically independent errors of x,y,z . . ., respectively. The error induced in u as a result of errors ε_1, ε_2, ε_3, . . . has a variance of

$$V(\delta) = \left(\frac{\partial f}{\partial x}\right)^2 V(\varepsilon_1) + \left(\frac{\partial f}{\partial y}\right)^2 V(\varepsilon_2) + \ldots . \tag{A-11}$$

The partial derivations are evaluated at values equal or close to the measured values of (x,y,z, . . .). If $\varepsilon_1 \sim N(0, \sigma_x^2)$, $\varepsilon_2 \sim N(0, \sigma_y^2)$, etc., then Eq. (A-11) can be written as

$$V(\delta) = \left(\frac{\partial f}{\partial x}\right)^2 \sigma_x^2 + \left(\frac{\partial f}{\partial y}\right)^2 \sigma_y^2 \ldots . \tag{A-12}$$

APPENDIX B

APPROXIMATE AVERAGE VALUE AND VARIANCE OF AN ARBITRARY FUNCTION

To find the exact mean and variance of an arbitrary function of several random variables is usually a very difficult task. However, if the function varies slowly in the region where the values of the independent variables remain within one or two standard deviations of their mean, the function can adequately be represented by the linear terms of its Taylor series expansion.

Let $u = f(x,y)$, where x and y are random variables with mean values $\bar{x}$ and $\bar{y}$, variances σ_x^2 , σ_y^2 and covariance σ_{xy}. Let

$$x = \bar{x} + e_x \tag{B-1}$$

and

$$y = \bar{y} + e_y \tag{B-2}$$

where the random errors e_x and e_y are assumed distributed $N(0, \sigma_x^2)$ and $N(0, \sigma_y^2)$. If we expand u about the point $\bar{x}$ and $\bar{y}$, and retain only the linear terms, then

$$u \cong f(\bar{x},\bar{y}) + \frac{\partial f}{\partial x}(x - \bar{x}) + \frac{\partial f}{\partial y}(y - \bar{y}) \tag{B-3}$$

where the partial derivatives with respect to x and y are evaluated at the point $(\bar{x}, \bar{y})$.

The expected or mean value of u is given by

$$E[u] \cong f(x,y) \tag{B-4}$$

since

$$E[x - \bar{x}] = E[e_x] = 0 \tag{B-5}$$

and

$$E[y - \bar{y}] = E[e_y] = 0 \quad . \tag{B-6}$$

The variance of u is

$$V[u] = \left(\frac{\partial f}{\partial x}\right)^2 \sigma_x^2 + \left(\frac{\partial f}{\partial y}\right)^2 \sigma_y^2 + 2 \left(\frac{\partial f}{\partial x}\right)^2 \left(\frac{\partial f}{\partial y}\right)^2 \sigma_{xy} \tag{B-7}$$

since the variance of a constant (i.e., $f(\bar{x},\bar{y})$ is zero. If x and y are independent random variables, then the covariance is zero.

APPENDIX C

IMAGE LOCATION EQUATIONS EMPLOYING A MOVING SOURCE

The analysis that follows is similar to the approach used by Champagne and Hildebrand.[13,14] Figure 1 is a simplified diagram to provide the terminology and geometry for the derivation of the image equations.

The phase at the receiver point (x,y,z) during the acoustic hologram construction is

$$\Phi(x,y,z) = \phi_o(x,y,z) - \phi_r(x,y,z) \tag{C-1}$$

where

$$\Phi(x,y,z) = \frac{2\pi}{\lambda_S}\left[r_1 + r_0 - r_2\right] \quad . \tag{C-2}$$

The phase at the receiver point (x,y,z) after the hologram is illuminated by the reconstruction source

$$\Phi_1(x,y,z) = \pm\frac{2\pi}{\lambda_S}\left[r_1 + r_0 - r_2\right] - \frac{2\pi}{\lambda_L} r_a \tag{C-3}$$

where

λ_S = acoustic wave length in the construction medium,

λ_L = reconstruction (light) wave length, and

+ sign refers to the conjugate image,

- sign refers to the real image.

If the phase front (C-3) is to focus at the image point (x_b, y_b, z_b), then

$$\Phi_1(x,y,z) = \frac{2\pi}{\lambda_L} r_b \tag{C-4}$$

where this is termed the Gaussion image sphere. The usual procedure is to expand the distance terms (r_a, r_b, r_1, r_2 and r_0) in a binomial

series and equate coefficients of x,y and z. We expand the distance terms about the origin of the (x,y,z) system and the distance r_0 is expanded about the α,β,γ system. The area in which the receiver scans is assumed small with respect to the distances and is centered at the (x,y,z) origin. A similar restriction holds for the source motion. Then we have

$$\Phi_1(x,y,z) = \pm\frac{2\pi}{\lambda_S}\left\{r_1 - \frac{xx_1}{r_1} - \frac{yy_1}{r_1} + \frac{x^2}{2r_1} + \frac{y^2}{2r_1} + r_0 - \frac{x_1\alpha}{r_0} - \frac{y_1\beta}{r_0}\right.$$

$$\left. + \frac{\alpha^2}{2r_0} + \frac{\beta^2}{2r_0} - r_2 + \frac{x_2x}{r_2} + \frac{y_2y}{r_2} - \frac{x^2}{2r_2} - \frac{y^2}{2r_2} + \cdots\right\} - \frac{2\pi}{\lambda_L}\left\{r_a - \frac{x_ax}{r_a}\right.$$

$$\left. - \frac{y_ay}{r_a} + \frac{y^2}{2r_a} + \frac{x^2}{2r_a} + \cdots\right\} = \frac{2\pi}{\lambda_L}\left\{r_b - \frac{x_bx}{r_b} + \frac{x^2}{2r_b} + \cdots\right\} \qquad \text{(C-5)}$$

The simulated receiver position (ξ,η) can be defined in terms of the actual and simulated velocities V_x, V_y, V_ξ, V_η, where

$$\xi = \frac{V_\xi}{V_x}x \qquad \text{(C-6)}$$

and

$$\eta = \frac{V_\eta}{V_y}x \qquad \text{(C-7)}$$

After substituting Eqs. (C-6) and (C-7) into Eq. (C-5) and retaining only the first two terms of the expansion, we have:

$$\Phi_1(x,y,z) = \frac{2\pi}{\lambda_S}\left\{r_1 - \frac{V_x}{V_\xi}\xi\frac{x_1}{r_1} - \frac{V_y}{V_\eta}\eta\frac{y_1}{r_1} + \left(\frac{V_x}{V_\xi}\right)^2\xi^2\frac{1}{2r_1} + \left(\frac{V_y}{V_\eta}\right)^2\eta^2\frac{1}{2r_1}\right.$$

$$\left. + r_0 - \frac{(x_1 - x_0)\alpha}{r_0} + \frac{(y_1 - y_0)\beta}{r_0} + \frac{\alpha^2}{2r_0} + \frac{\beta^2}{2r_0} - r_2^2 + \frac{V_x}{V_\xi}\xi\frac{x_2}{r_2} + \frac{V_y}{V_\eta}\eta\frac{y_2}{r_2}\right.$$

$$- \left(\frac{V_x}{V_\xi}\right)^2 \xi^2 \frac{1}{2r_2} + \left(\frac{V_y}{V_\eta}\right)^2 \eta^2 \frac{1}{2r_2} \Bigg\} - \frac{2\pi}{\lambda_L} \left\{ r_a - \frac{V_x}{V_\xi} \xi \frac{x_a}{r_a} - \frac{V_y}{V_\eta} \eta \frac{y_a}{r_a} \right.$$

$$\left. + \left(\frac{V_y}{V_\eta}\right)^2 \eta^2 \frac{1}{2r_a} + \left(\frac{V_x}{V_\xi}\right)^2 \xi^2 \frac{1}{2r_a} \right\} = \frac{2\pi}{\lambda_L} \left\{ r_b - \frac{V_x}{V_\xi} \xi \frac{x_b}{r_b} - \frac{V_y}{V_\eta} \eta \frac{y_b}{r_b} \right.$$

$$\left. + \left(\frac{V_x}{V_\xi}\right)^2 \xi^2 \frac{1}{2r_b} + \left(\frac{V_y}{V_\eta}\right)^2 \eta^2 \frac{1}{2r_b} \right\} \quad . \tag{C-8}$$

If we allow only parallel motion of the source and receiver, then the expressions for the source position are:

$$\alpha = a_0 + a_1 x \quad , \tag{C-9}$$

$$\beta = b_0 + b_1 y \quad . \tag{C-10}$$

The velocities of the source and receiver are related by

$$\frac{d\alpha}{dt} = a_1 \frac{dx}{dt} \quad , \qquad \frac{d\beta}{dt} = b_1 \frac{dy}{dt} \tag{C-11}$$

where $\frac{d\alpha}{dt}$, $\frac{d\beta}{dt}$ and $\frac{dx}{dt}$, $\frac{dy}{dt}$ are the velocity components of the source and receiver, respectively. The final expressions for α and β (assuming $a_0 = b_0 = 0$) are

$$\alpha = \frac{V_{0\alpha}}{V_\xi} \xi \quad , \tag{C-12}$$

$$\beta = \frac{V_{0\beta}}{V_\eta} \eta \quad . \tag{C-13}$$

IMAGE LOCATION EQUATIONS

After substituting Eqs. (C-12) and (C-13) into Eq. (C-8) and equating like coefficients, we obtain the following expressions for image location:

$$\frac{x_b}{r_b} = \pm \frac{\lambda_L}{\lambda_S} \frac{V_x}{V_\xi} \left\{ \frac{x_1}{r_1} + (x_1 - x_0) \frac{V_{0\alpha}}{V_x} \frac{1}{r_0} - \frac{x_2}{r_2} \right\} - \frac{x_a}{r_a} \quad , \tag{C-14}$$

$$\frac{y_b}{r_b} = \pm \frac{\lambda_L}{\lambda_S} \frac{V_y}{V_\eta} \left\{ \frac{y_1}{r_1} + (y_1 - y_0) \frac{V_{0\beta}}{V_y} \frac{1}{r_0} - \frac{y_2}{r_2} \right\} - \frac{y_a}{r_a} \quad , \tag{C-15}$$

$$\frac{1}{r_b} = \pm \frac{\lambda_L}{\lambda_S} \left(\frac{V_x}{V_\xi} \right)^2 \left\{ \frac{1}{r_1} + \left(\frac{V_{0\alpha}}{V_x} \right)^2 \frac{1}{r_0} - \frac{1}{r_2} \right\} - \frac{1}{r_a} \quad , \tag{C-16}$$

$$\frac{1}{r_b} = \pm \frac{\lambda_L}{\lambda_S} \left(\frac{V_y}{V_\eta} \right)^2 \left\{ \frac{1}{r_1} + \left(\frac{V_{0\beta}}{V_y} \right)^2 \frac{1}{r_0} - \frac{1}{r_2} \right\} - \frac{1}{r_a} \tag{C-17}$$

In order for r_b to be the same for each coordinate (i.e., stigmatic), then the following conditions must be satisfied

$$\frac{V_x}{V_\xi} = \frac{V_y}{V_\eta} \tag{C-18}$$

and

$$\frac{V_{0\alpha}}{V_x} = \frac{V_{0\beta}}{V_y} \tag{C-19}$$

Then we have the final expressions for the image location equations

$$\frac{x_b}{r_b} = \pm \frac{\lambda_L}{\lambda_S} g \left\{ \frac{x_1}{r_1} + (x_1 - x_0) \frac{f}{r_0} - \frac{x_2}{r_2} \right\} - \frac{x_a}{r_a} \quad , \tag{C-20}$$

$$\frac{y_b}{r_b} = \pm \frac{\lambda_L}{\lambda_S} g \left\{ \frac{y_1}{r_1} + (y_1 - y_0) \frac{f}{r_0} - \frac{y_a}{r_2} \right\} - \frac{y_a}{r_a} \quad , \tag{C-21}$$

$$\frac{1}{r_b} = \pm \frac{\lambda_L}{\lambda_S} g^2 \left\{ \frac{1}{r_1} + \frac{f^2}{r_0} - \frac{1}{r_2} \right\} - \frac{1}{r_a} \quad , \tag{C-22}$$

where

$$g = \frac{V_x}{V_\xi} = \frac{V_y}{V_\eta} \tag{C-23}$$

and

$$f = \frac{V_{0\alpha}}{V_x} = \frac{V_{0\beta}}{V_y} \tag{C-24}$$

MAGNIFICATIONS

Lateral Magnification

$$M_L(x) = \frac{\partial x_b}{\partial x_1} = \pm \frac{\lambda_L}{\lambda_S} g \left\{ 1 + \frac{r_1 f}{r_0} \frac{r_b}{r_1} \right\} \quad , \tag{C-25}$$

$$M_L(y) = \frac{\partial y_b}{\partial y_1} = \pm \frac{\lambda_L}{\lambda_S} g \left\{ 1 + \frac{r_1 f}{r_0} \frac{r_b}{r_1} \right\} \quad , \tag{C-26}$$

where

$$z_1 >> x_1 \text{ or } y_1$$

$$z_1 - z_0 >> x_1 - x_0 \text{ or } y_1 - y_0 \quad .$$

If the source and the receiver are located at the same position (i.e., $r_1 = r_0$ and $f = 1$), then the lateral magnification can be expressed by the following equation:

$$M_L(x) \cong M_L(y) = \pm 2 \frac{\lambda_L}{\lambda_S} \frac{r_b}{r_1} g \quad . \tag{C-27}$$

Radial Magnification

$$M_R = \pm \frac{\lambda_L}{\lambda_S} \left(\frac{r_b}{r_1} g \right)^2 \left[1 + f^2 \left(\frac{r_1}{r_0} \right)^2 \right] \quad . \tag{C-28}$$

If the magnification of the hologram is to be undistorted, then the ratio M_R/M_L must equal unity:

$$\frac{M_R}{M_L} = g \frac{r_b}{r_1} \left[\frac{1 + f^2 \left(\frac{r_1}{r_0} \right)}{1 + f \left(\frac{r_1}{r_0} \right)} \right] \quad . \tag{C-29}$$

The ratio of the magnifications can be controlled by the velocity ratios

$$\left(f = \frac{V_{0\alpha}}{V_x} = \frac{V_{0\beta}}{V_y} \right) \quad .$$

Scanning the receiver and source together the ratio reduces to the following expression:

$$\frac{M_R}{M_L} = g \frac{r_b}{r_1} \left[\frac{1 + f^2}{1 + f} \right] \quad . \tag{C-30}$$

APPENDIX D

HOLOGRAPHIC SIGNAL PROCESSING

The reference signal can be written as: $\alpha = A \cos(\omega t + \phi_r)$, and the object signal expressed as: $\beta = B(x,y) \cos[\omega t + \phi_o(x,y)]$ where $(\phi_r - \phi_o)$ represents the phase difference between the signals:

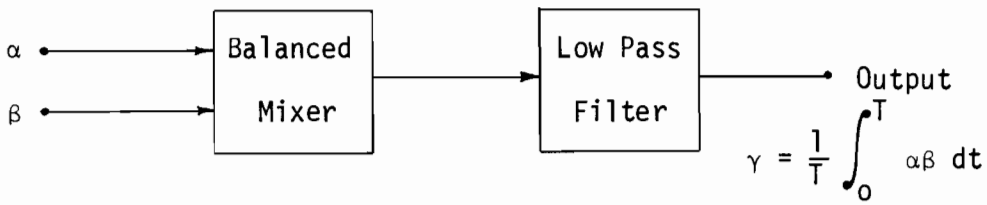

$$\gamma = \frac{1}{T}\int_0^T AB(x,y) \cos[\omega t + \phi_r] \cos[\omega t + \phi_o(x,y)] \, dt$$

Let

$$\tau_1 = \omega t + \phi_r \quad ,$$

$$\tau_2 = \omega t + \phi_o$$

then

$$\cos\tau_1 \cos\tau_2 - \sin\tau_1 \sin\tau_2 = \cos(\tau_1 + \tau_2) \quad ,$$

$$\cos\tau_1 \cos\tau_2 + \sin\tau_1 \sin\tau_2 = \cos(\tau_1 - \tau_2) \quad ,$$

$$\cos\tau_1 \cos\tau_2 = 1/2 \cos(\tau_1 + \tau_2) + 1/2 \cos(\tau_1 - \tau_2) \quad ,$$

$$\gamma = \frac{1}{T}\int_0^T \frac{AB}{2} \cos(2\omega t + \phi_r + \phi_o) \, dt + \frac{1}{T}\int_0^T \frac{AB}{2} \cos(\phi_r - \phi_o) \, dt \quad ,$$

$$\gamma = \frac{1}{T}\int_0^T \frac{AB}{2} \cos(\phi_r - \phi_o) \, dt = \frac{AB}{2} \cos[\phi_r - \phi_o]$$

where ϕ_r = constant,

$\phi_o = f(x,y)$ only .